Australian Government
Bureau of Rural Sciences

Developing a salt source model for the Murray-Darling Basin from natural soil-radioactivity and geological data

P.N. Bierwirth and R.S. Brodie

Postal address:
Bureau of Rural Sciences
GPO Box 858
Canberra, ACT 2601

Email: salesbrs@brs.gov.au

Internet: http://www.affa.gov.au/brs

Copies available from:
BRS Publication Sales
GPO Box 858
Canberra ACT 2601
Ph: 1800 020 157
Fax: 02 6272 2330

Executive Summary

This report presents a new technique for mapping regional salt-sources that has major implications for salinity management. This mapping was done by analysing a regional mosaic of airborne gamma-radiometrics together with existing airborne geophysics and drilling data collected as part of the Murray Darling Basin (MDB) airborne geophysics project.

A significant correlation was found between aeolian (wind-blown) materials, upland salts and the geophysical signatures of both airborne gamma-radiometrics and airborne electromagnetic (AEM) data. This is consistent with the conceptual model that much of the salt in the upland areas of the MDB is sourced from deposited aeolian materials that have been derived from deflationary events in salt-bearing landscapes in the western arid part of the basin. Drillhole data from multiple source areas and identification from other work suggests a characteristic gamma-radiometric signature for aeolian salt-sources. This signature was used as a target and the Euclidean distance from this target was derived for each pixel in the MDB radiometrics mosaic (using both potassium and thorium components) to form a continuous classification of upland salt-source.

The major area of saline aeolian materials forms a fragmented arcuate body stretching from northern Victoria to north-central NSW that is consistent with aeolian deposition from a dominant westerly dust path. Much of the modelled salt-sources lie in a broad region with geomorphic similarity in the lower western slopes of the Great Dividing Range.

The combined modelling and analysis of AEM and gamma-ray data provides a better understanding of salinity in relation to geological materials in the landscape. The upland aeolian salt source model, based on radiometric potassium (K) and thorium (Th) logically correlates with the uppermost AEM layers. The difference is that the gamma model is detecting the original source materials while the AEM shows the location of the salt, including where it has been subsequently transported. This means that the AEM can now be better separated into components of salt-source and salt mobilisation.

In terms of management, the new model and the derived salt source mapping adds an extra dimension to existing geophysical techniques. The radiometrics data is widely available, so the technique is a cost-effective addition to the current tools. Unlike AEM, this is a method that can be readily and synoptically applied over large areas.

Contents

Figures

1. Introduction

Dryland salinity is recognised as a major problem in the Australian landscape affecting both economic productivity and biodiversity. Although surface salinisation has been readily identified in numerous catchments, the scope of the problem, future risk and management options are less clear. Much recent work has focussed on identifying the location of salt stores and mobility pathways using geophysical data, particularly Airborne Electromagnetic (AEM) surveys (Dent, 2003). Although powerful as a management and information gathering tool, AEM does not differentiate between mobilised salt and areas that are salt-sources. Identifying and mapping these salt sources is fundamental for salinity management yet has not been achieved at the regional or catchment scale.

In the southeastern uplands of the Murray-Darling Basin, a common conception has been that salt is sourced from the whole landscape, being present in the overall geology or groundwater systems. This includes connate salts coincident with deposition (as in marine sediments) or salts derived from subsequent weathering processes. More recently, it has become accepted that salts have been introduced to the landscape rather than being derived in situ from bedrock. This can be by rainfall accessions with evapotranspiration causing accumulation of oceanic cyclic salts in the soil profile. Salts can also be associated with silty clay deposits derived from wind-blown sources. This mechanism of aeolian deposition of salts as outlined in previous studies such as Bowler (1983), Acworth *et al* (1997) and Evans (1998) is the focus of this report. A new mapping technique, utilising airborne gamma-radiometrics, for locating aeolian salt sources is presented and validated by comparisons with other datasets in specific catchments. The regional identification of extensive deposits of near-surface saline aeolian material has significant implications in terms of the focussing of effort for salinity management.

2. Landscape Salt Sources in Aeolian Deposits

It is widely accepted that salts have been introduced to the landscape rather than being derived from in situ bedrock sources (Evans, 1998). The combination of a saline arid inland and a history of dominant westerly winds suggest that wind-borne (aeolian) deposition of clay and salt is significant for the southeastern upland margins of the Murray-Darling Basin. Such surficial deposits can be the dominant source of salt in these catchments and when saturated or mobilised become a driver for dryland salinity.

2.1 Aeolian deposits and their occurrence in the Murray-Darling Basin

Previous investigations have shown that extensive deposits of aeolian material occur in the landscape of southeastern Australia. The term 'parna', which is the aboriginal word for dust, was initially used to describe aeolian clay deposits in the Riverine Plain (Butler, 1956, Butler and Hutton, 1956). Similar deposits have been identified in the vicinity of Griffith (van Dijk, 1958), Swan Hill (Churchward, 1963) and Wagga Wagga (Beattie, 1972). Further to the east, aeolian contributions to the soil profile have been found near Blayney (Dickson and Scott, 1998), as well as Young, Canberra and Bemboka (Chartres *et al*, 1988). Mixtures of aeolian and colluvial material have been identified in valley floors in the Yass catchment (Acworth *et al*, 1997). Chartres and Chivas (1987) estimated that about half of the Southern Tablelands soil on granite is dust-derived. Aeolian dust has been found in the alpine humus soil profiles of the Main Range of Kosciusko National Park (Johnston, 2001).

Various lines of evidence have been used in these studies to cite an aeolian origin including:

(i.) The uniformity of the profile which overly different geological units in various topographic settings. An erosional unconformity with the underlying bedrock can be observed (Acworth *et al*, 1997);
(ii.) A bi-modal particle size distribution with peaks in the clay and coarse silt fractions;
(iii.) Contrasts in soil chemistry and mineralogy when compared with underlying geological material e.g. oxygen isotope abundance in quartz grains (Chartres *et al*, 1988) or the presence of smectite clays (Acworth *et al*, 1997);
(iv.) The presence of soil carbonates; and
(v.) Soil sub-plasticity.

For example, at Wagga Wagga, the aeolian dust deposits are often red clays that form a continuous mantle, particularly in high plains (Chen, 2001). These soils have the characteristic bi-modal particle distribution, with one mode in course silt (4-6 Phi) and the other in clay (Chen, 2001). In the floodplains, the red clay is basically absent although aeolian materials are likely to be present mixed with recent sediments. On hills with average slope exceeding 30%, the red clay contains significant amounts (up to >50%) of gravels (i.e. mixed with locally derived colluvium) and exists only at lower and foot-slopes (Chen, 2001). On hills with average slopes of 10–30%, mixed colluvium/ aeolian and blanket aeolian may alternately occur.

This is similar to the landscape in the Billabong Creek catchment (McKenzie and Gallant, 2005), refer Figure 1. Exposures suggest that about 5-7 metres of aeolian material has been deposited over the flatter parts of the catchment. Drillcore from the area has been analysed using laser grainsize analysis (Jones *et al*, 2003). One of these holes (BC17) intersected 14 metres of saline cover sediments overlying granite saprolite and the results of the grainsize analysis are shown in Figure 2. A bi-modal distribution is evident, with the second grainsize peak in the range 0.0078 – 0.0156 mm being fine silt sized particles. This is equivalent to 6-7 Phi and, significantly, this relates to the mean grainsize for modern day dust (6.6 - 6.8 Phi) (Melis and Acworth, 2001).

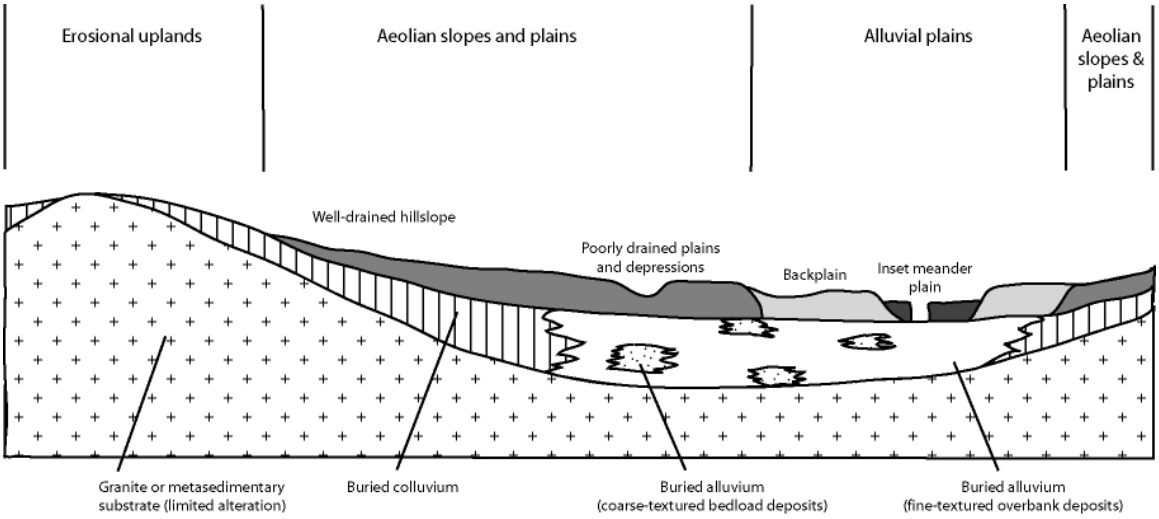

Figure 1: Idealized cross-section of geomorphic units in the Billabong Creek catchment, including aeolian-derived material (From McKenzie and Gallant, 2005)

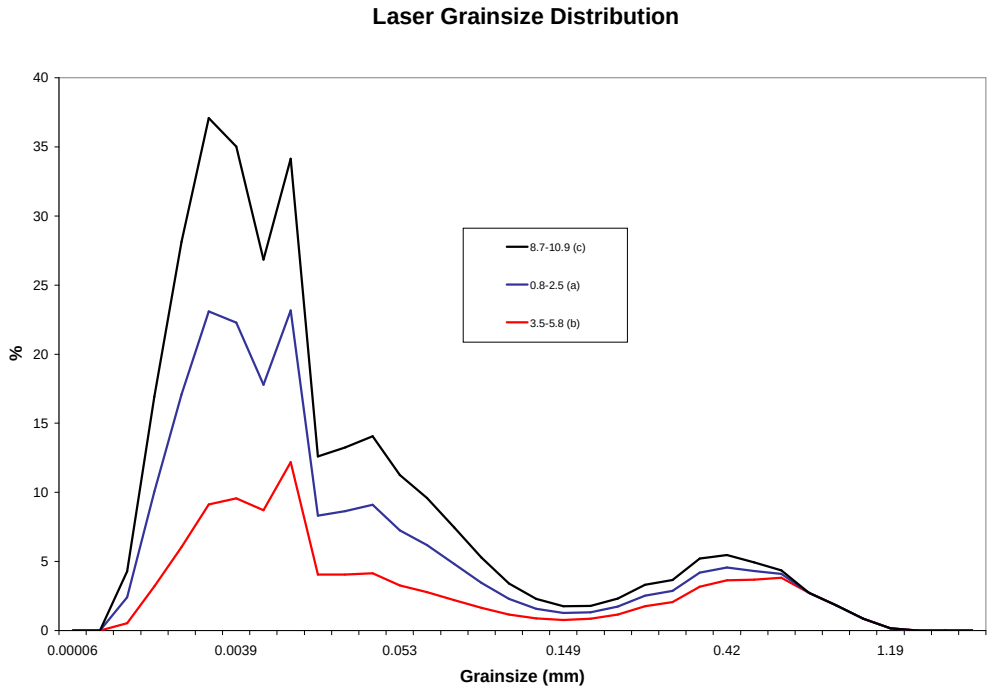

Figure 2: Laser grainsize analysis of covering sediments in borehole BC 17d (Jones *et al*, 2003).

2.2 Aeolian depositional processes

The arid interior of Australia consists of desert landforms such as dunefields and playa lakes which are a vast reservoir of dust material and salt. Episodic dust storms originating from inland areas are vectors for sediment transport. In southeastern Australia, the major wind systems are to the east, enabling aeolian deposition on the eastern flanks of the Murray-Darling Basin and beyond (Greene *et al*, 2001), refer Figure 3. The sediment loads associated with these events can be significant. A dust storm in December, 1987 was estimated to have eroded 5.5-6.3 million tonnes from its original provenance in western Queensland (Knight *et al*, 1995). Subsequent dust deposition over the 24-hour period was measured at sites to be 2 tonnes/km^2/d, compared with the annual average rate of 5-10 tonnes/km^2/yr in Adelaide. About 1.9-3.4 million tonnes left the Australian continent, and on the Southern Alps in New Zealand, the dust storm tinged the snow red. Although severe, such a storm would be considered to be a 1 in 20 year event based on the historic record since the 1900s. By accounting for the frequency and magnitude of dust storm events, Knight *et al* (1995) estimated the annual sediment yield from the western Queensland source region to be 107-122 tonnes/km^2/yr. By comparison, the sediment load estimated for all Australian rivers is about a third of this rate, at 32-45 tonnes/km^2/yr (Olive and Walker, 1982).

Paleoenvironmental studies of Quaternary landforms and sequences suggest that such processes and dust paths have persisted over the past 500,000 years (Bowler, 1976; McTainsh, 1989). This relates to a transition to more arid conditions from that time which has been established through investigations at sites across Australia (Figure 4).

For example, Lake Bungunnia was formed in the Murray Geological Basin during the Late Pliocene (~2.4 Ma) by tectonic uplift in the Padthaway region of South Australia. This large ancient lake covering an area of 33,000 km^2 (Stephenson, 1986) was fed by the Murray-Darling river system (Figure 6) with flows considerably greater than the modern regime. This period is represented by extensive deposits of sandy, micaceous clays (Blanchetown Clay) containing evidence of freshwater ecology. The onset of arid conditions is reflected in overlying gypsiferous evaporitic sediments indicating hypersaline conditions as well as aeolian sands (Figure 4). These deposits and their modern equivalents represent a major reservoir of clays and salt that was made available for aeolian transport eastwards by prevailing winds (Stephenson, 1986). The extent of the dunefields of the Mallee region provides testament to the dominance of aeolian processes since the demise of Lake Bungunnia (Figure 5). These dunefields can also be viewed as the proximal coarser equivalents of the distal finer aeolian deposits found in the upland areas to the east. Dune profiles contain calcareous soil horizons or calcretes that show a history of remobilisation and stabilisation relating to climate oscillations (Brown and Stephenson, 1991). Lunettes or source-bordering dunes are evident on the eastern margins of the playa lakes, associated with the remnants of Lake Bungunnia, formed by the predominately westerly winds. These dunes can contain sand layers that indicate deflation of lake shore beaches during wetter periods as well as clay pellet layers which indicate deflation of saline lake floors during transitional climate phases (Bowler and Wasson, 1984).

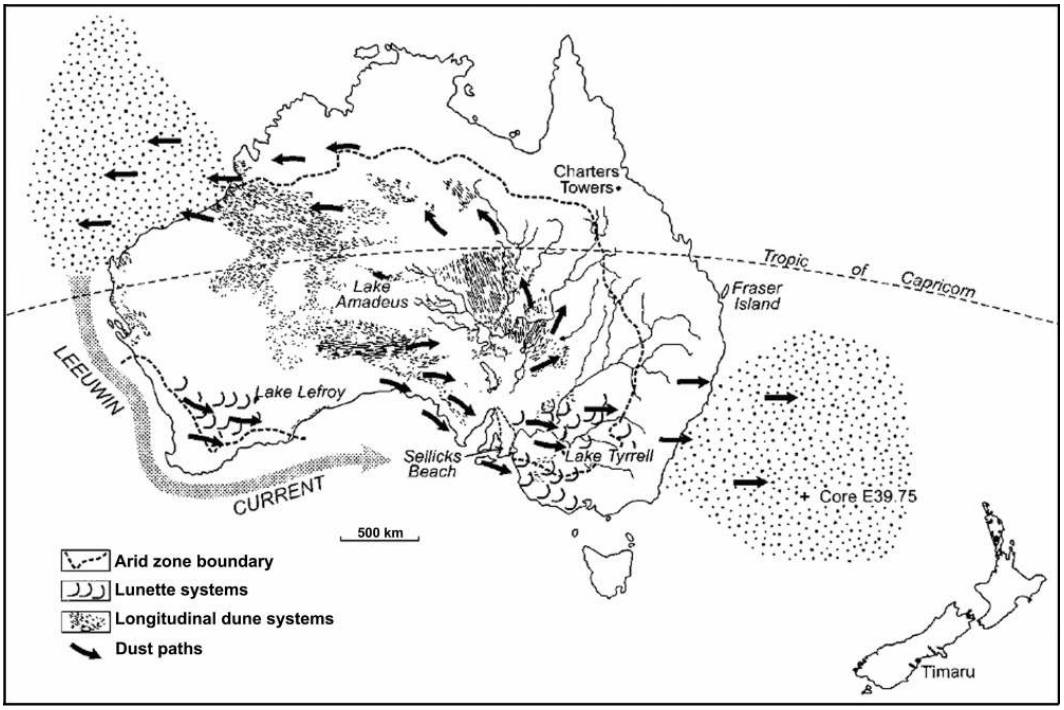

Figure 3. Arid-zone boundary, lunette zones, dune systems and dust paths after Bowler (1976) and McTainsh (1989). Figure from Pillans and Bourman, 2001.

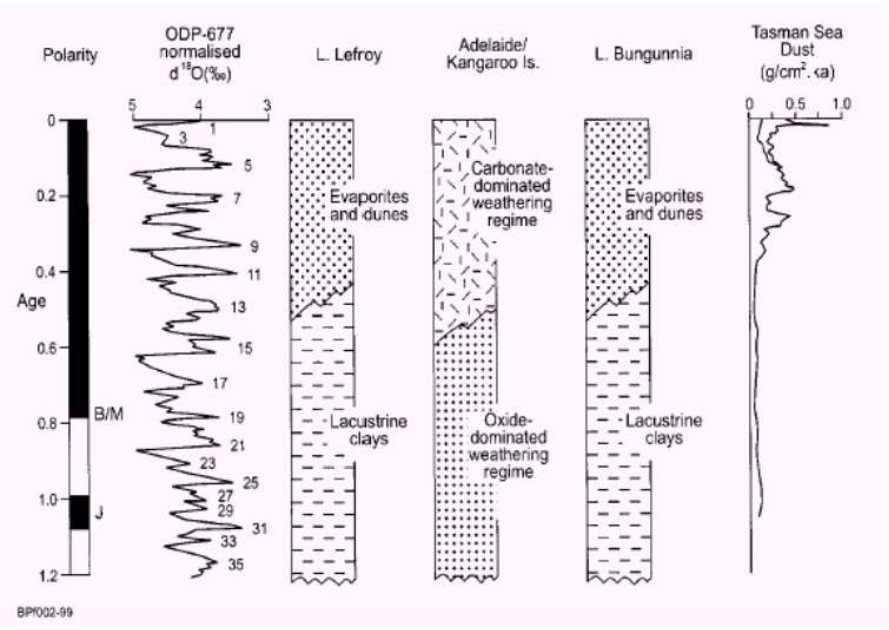

Figure 4: Summary of paleoclimatic records in southern Australia showing mid-Pleistocene arid shift. Adelaide/Kangaroo Is. (Pillans and Bourman 1996), Lake Bungunnia (An *et al*. 1986), Lake Lefroy (Zheng *et al.* 1998), Tasman Sea dust (Hesse 1994), ODP Site 677 (Shackleton *et al*. 1990) – Figure from Pillans and Bourman, 2001.

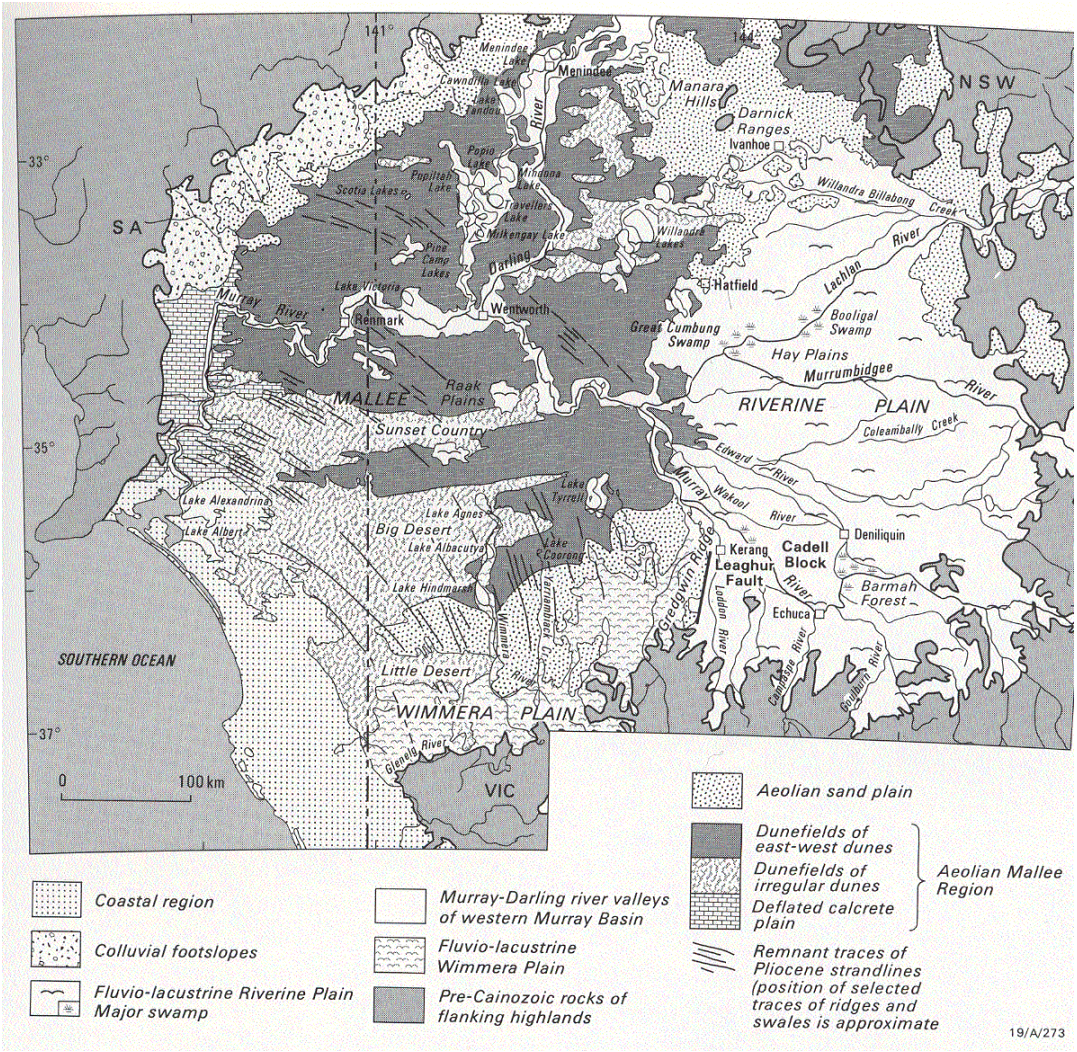

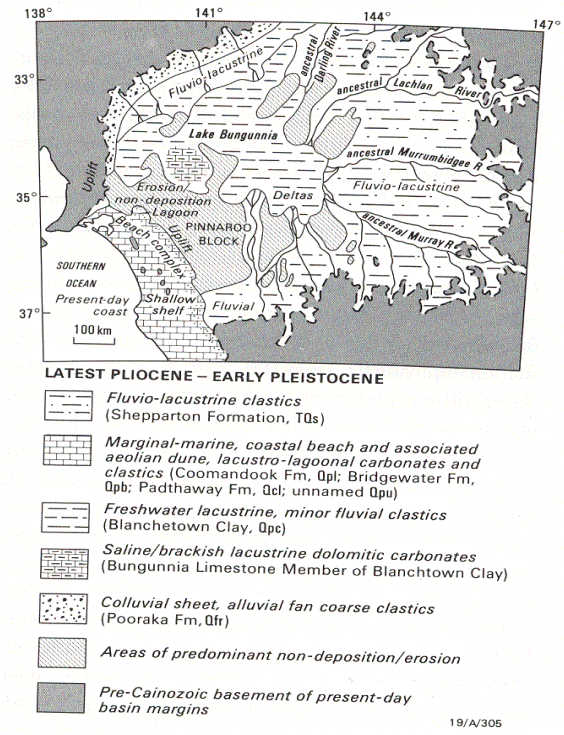

Figure 5:(above): Geomorphic regions of the Murray Geological Basin showing extensive aeolian landforms (from Brown and Stephenson, 1991)

Figure 6: (left) Late Pliocene to Early Pleistocene (2.5-0.7 Ma) paleogeography of the Murray Geological Basin, showing extent of ancient Lake Bungunnia (from Brown and Stephenson, 1991)

Analyses of offshore sediment cores in the Tasman Sea provide a more detailed record of changes in the dust flux and relationships with the paleoclimatic record (Hesse, 1994), refer Figure 4. These cores confirm the onset of aridity albeit at about 350,000 years ago, with periods of higher dust flux relating to glacial periods. Vegetation reconstructions for these periods suggest retreat of woodland and forest to narrow coastal margins, with expansion of semi-arid savannah or grassland and therefore a greater source area for dust (Hope, 1987). The spatial extent of the dust plume in the ocean floor sediments is consistent with the model of prevailing wind systems for southeastern Australia (Figure 3). On this basis, Hesse (1994) inferred that the dominant source area for the dust path was the Murray-Darling Basin and Lake Frome Basin. Interpretation of uranium-lead dating of detrital zircon in samples of dust-dominated soils at Blayney and Tumbarumba came up with similar conclusions (Gatehouse *et a*l, 2001). The zircon age patterns from these samples in the eastern highlands were very similar to the signature found in the Mallee dunefield further inland in the Murray Geological Basin.

2.3 Aeolian deposits as a salt store

The coincidence of salt and clays in these inland arid source areas suggest that aeolian materials are often sources of salts. It has been postulated that salt accompanying dust derived from the Murray Geological Basin is the principal source of salts found in the uplands region of the Murray-Darling Basin (Bowler, 1983). For example, this mechanism was inferred to have caused salt accumulation in the soil profile at Lake George since about 270,000 years ago, and reflected in a transition in dominant vegetation from *Casuarina* to *Eucalyptus* (Crowley, 1994). This salt transport is particularly the case during periods of high groundwater levels and active deflation of the extensive deposits of saline lacustrine clays evident in the Murray Basin. This represents an eastwards wind-borne export of salt that is opposite to the export westwards by the stream network.

Investigations in some of the southeastern upland catchments of the Murray-Darling Basin provide evidence for the linkage between aeolian deposits and salt. In the Boorowa catchment, the majority of salt is concentrated in the shallow soil/regolith profile which was inferred to have an aeolian component (Evans, 1998). In the more subdued upper parts of the catchment, the shallow-channelled streams are in contact with these surficial deposits and have relatively high salt loads. Further down the catchment, the streams are incised into the underlying less-weathered fractured rock and receive fresher groundwater discharge. A connate origin of the salt from the Paleozoic marine fractured rocks is discounted by groundwater chlorine-36 analyses indicating that the stored salt is much younger than the rocks.

In the Yass River catchment, surficial deposits of smectite-rich silty clays with variable salt content have been interpreted as being aeolian in origin (Acworth *et al*, 1997). Several episodes of remobilisation of this material and mixing with colluvial material have been identified. These episodes may correlate with wetter periods in the Pleistocene allowing saturation of the dust profile and subsequent structural instability and failure as debris flows and land slips. Field mapping suggest a correlation between these deposits (which occur on the lower slopes and valley floors) and dryland salinity outbreaks. This was attributed to upward movement of groundwater from the underlying fractured rocks mobilising salt stored in the shallow debris flow deposit. In the absence of the clay debris flows, groundwater discharge as hillslope springs is not saline and can support small wetland ecosystems. Smectite-rich horizons within the debris flows are strongly dispersible and mobilisation of this material can contribute clay and salt to surface runoff and local streams (Melis and Acworth, 2001).

At Simmons Creek within the Billabong Creek catchment, NSW, English *et al* (2002) also suggest that significant salt storage relates to aeolian parna deposits. These reworked aeolian

deposits now blanket the topographically low parts of the catchment and correspond with low gamma-radiometric responses.

Relatively high salinity levels (63.5-230.5 EC) were found in surface horizons of Kosciusko alpine soil profiles inferred to have a significant dust component, compared with deeper in the profile (8.5-43.3 EC) where bedrock weathering processes dominate (Johnston, 2001).

Even in the present-day climate, saline dustfall (dry particulate grains of resuspended terrestrial dust with some entrained salt sourced) and dissolved salts in rainfall (principally sourced from the ocean) can be considerable. Modern dust may contain up to 50% by weight of salts (Kiefert, 1997). Comparison of cation ratios of sea water analyses with analyses of rainfall samples taken near Scone, NSW, suggests that addition of soluble material to rain by aeolian processes is significant (Elliot and Holman, 1985).

3. Mapping of Aeolian Salt Stores

A regional mapping technique based on the conceptual model of aeolian deposits being a significant source of salts in the eastern upland catchments of the Murray-Darling Basin has been developed. The method uses gamma-radiometric survey data to differentiate near-surface wind-blown material from other landscape components.

3.1 Application of gamma radiometrics

Airborne gamma-spectrometry (AGS) uses gamma-ray emission in multiple wavelengths to derive abundances of the major gamma-emitting elements of potassium (K), thorium (Th) and uranium (U). This provides spatial images of the geochemistry of the upper rock/soil layer to a depth of about 30-45cm. Although lacking in depth of penetration, the distribution of these element concentrations at the surface can often be related to subsurface properties (Bierwirth, 1996).

The source minerals for potassium (K) are feldspars and micas and their weathering products such as illite clays. Uranium (U) and thorium (Th) are present in significant quantities in accessory minerals. The spatial distribution within the landscape of K, U and Th and the decay products of U and Th are also a function of physical and chemical weathering processes as well as sediment transport processes. In terms of weathering, K is by far the more mobile of the elements, Th is more resistant to weathering and U is perhaps less well understood. The U image data is also often noisy due to low counts collected by airborne sensors. Gamma-radiometric image interpretation depends therefore on the primary mineral content and the weathering patterns of these minerals influenced by geomorphology.

3.2 Previous gamma-radiometric studies relating to salinity

In a detailed study of radiometrics at Kyeamba Creek near Wagga Wagga (Bierwirth, 1996), a relationship was observed between salt scalds and low K areas (Figure 7a). This area is contained within Ordovician metasediments where high K relates to bedrock signatures of the shallow lithosols. At the time it was thought that the low K was associated with areas of clay linked with increased weathering and salt accumulation. Soil samples largely from the upper landscape showed a relationship between high K signal and low levels of salt (EC 1:5) in the soil profile (Figure 7b).

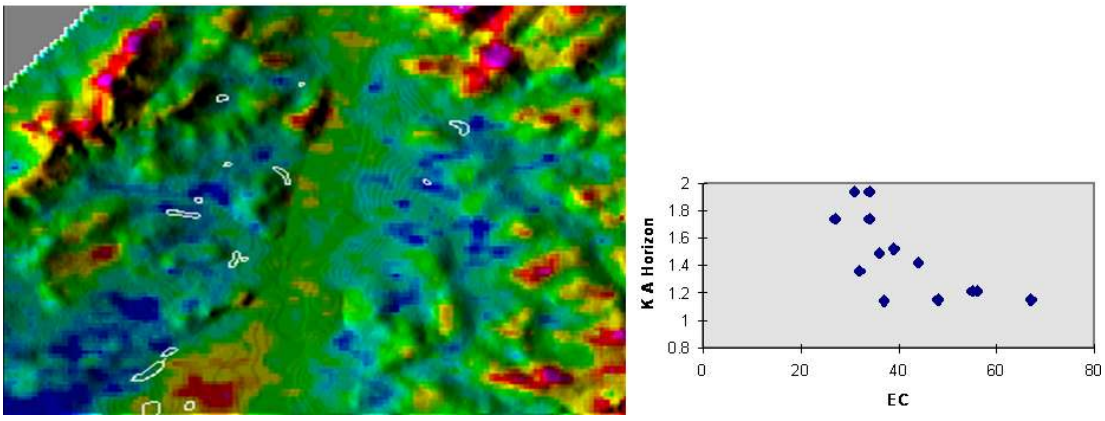

Figure 7: (a) Image of K draped on a shaded DEM at Kyeamba Creek, NSW. The white outlines are salt scalds and the image is 7 km across. Red areas are high values and blue is low. (b) soil sample measurements of total K in the A horizon expressed as percent versus EC 1:5 (uS/cm) from the B horizon..

Detailed soil sampling also showed that, in the metasediments, lower K is associated with increased weathering and depths of colluvium (Figure 8). The initial assumption was that the very low K areas were an extension of this phenomenon but reconsideration, based on the current work, suggests that the low-K response may represent introduced aeolian materials.

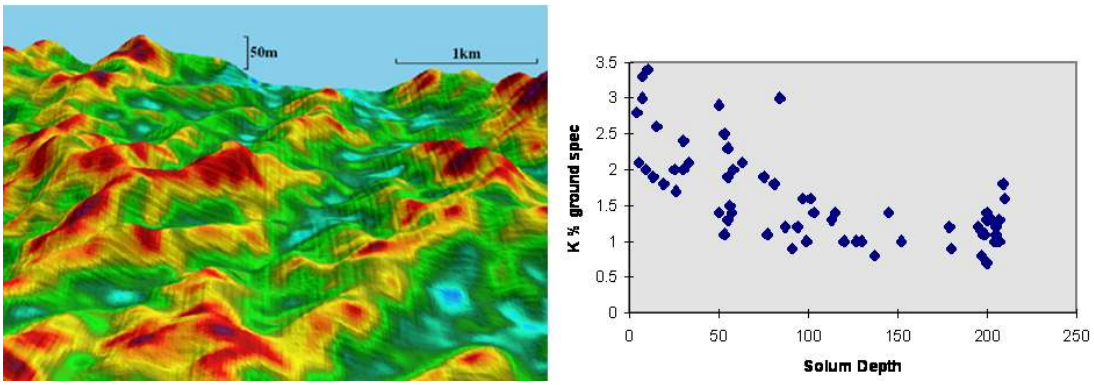

Figure 8: (a) 3-D perspective of K draped on a DEM for upland areas east of Kyeamba Creek, NSW. Red areas are high values and blue is low (b) solum depths (depth to saprolite) compared with K ground spectrometer measurements.

Following on from this work, Wilford *et al* (2001) attempted to relate low K to salt storage at Bethungra, NSW although their assumption was that salt was associated with clays in the weathered low-K soils. Although a loose relationship between landscape K and stream salinity was presented, an apparent relationship may be because these were residual landscapes likely to contain a significant component of aeolian materials. Wilford *et al* (2001) used a K-derivative image which adjusted K values for different lithologies and so is not appropriate for targeting the particular gamma-radiometric signature of blanketing aeolian materials. Also, the use of a single element can produce errors in any potential model due to low separability between aeolian soils and particular rocktypes such as quartz sandstones, limestones and basalts (Bierwirth, 2006).

In the Billabong Creek area, McKenzie and Gallant (2005) used airborne gamma K and topographic indices to map soil classes associated with aeolian materials. They concluded that units dominated by aeolian materials (Figure 1) were associated with low K (using uncalibrated data) and slopes less than 6 degrees. Another study by Dickson and Scott (1998) found that red aeolian soils in the Blayney district, NSW, had a characteristic gamma-radiometrics signature of 0.7% K, 2 ppm U and 11 ppm Th although there was no analysis of salt content.

Based on all previous work, there does appear to be a case for both aeolian sources of salt and the potential for gamma-radiometrics to identify these regionally. This is particularly the case in southeastern Australia where there is substantial evidence for westerly aeolian transport from a large reservoir of salt further inland for at least the last 350,000 years. The next steps are to acquire the necessary data, analyse these in relation to available borehole data and use this analysis to construct an appropriate model for spatially characterising salt sources in terms of aeolian soil profiles.

3.3 Data Acquisition

Airborne radiometrics data for the Murray-Darling Basin were downloaded via the internet from the Geophysical Archive Data Delivery (GADDS) system at Geoscience Australia. This included image data of the three gamma emitting elements (K, Th and U) for 94 individual airborne surveys. The gridded pixel size for these surveys ranged from 10m to 130m and these corresponded to flight line spacings ranging from 50m to 400m. A mosaic, with a pixel

size of 100m, was created for each of the three elements over the spatial extent of the basin. There were a number of issues with the collation of the mosaic. For example, a proportion of these surveys were represented in counts per second and not calibrated to element concentrations. This meant that these surveys had to be edge-matched to calibrated surveys. This was effective for the K data, but after compiling the mosaic it was clear that, for Th and U, even the calibrated data had level differences that were clearly evident at the survey boundaries. In most cases the calibration differences are due to the methods used by the various acquisition system operators. The errors are often produced by the use of inadequate calibration targets and in most cases the error translates to the sensitivity constant multiplier (B. Minty, *pers. com.*). As a consequence, the thorium data was then visually manipulated so that the smallest number of individual surveys was adjusted to produce an edge-matched mosaic.

Digital geology for the Murray-Darling Basin has previously been collated and simplified (Kingham, 1998). This was compiled from existing 1:250,000 and 1:100,000 scale geological mapping and provides simplified litho-stratigraphic groupings. Fundamental surficial geology is likely to be important when considering gamma-ray signatures and their relationship with surface materials.

3.4 Data Analysis

Analysis of borehole data

As mentioned previously, any salt-source model derived from the gamma-radiometrics should be based on field evidence. As part of the MDBC airborne geophysics project (Dent *et al*, 2003) a series of bores were drilled with the aim of verifying and calibrating airborne EM data-sets. Samples from these bores, often drilled through to basement rocks, were analysed for geophysical and chemical properties including salt (EC 1:5 soil extracts). This data can be used to assess landscape relationships between salt distribution and the gamma-radiometrics data.

Use of MRVBF to delineate upland holes

Alluvial areas may often have accumulated salts sourced from upland areas (Bierwirth, 2006). Therefore the gamma-ray signatures of alluvial materials will not necessarily relate to the original salt source. However in upland areas there is more likely to be a correlation between the gamma-radiometrics and salt, where salt-bearing sources and relatively salt-free areas are present. Selection of upland boreholes for further analysis was based on the Multi-Resolution Valley Bottom Flatness (MRVBF) index (Gallant and Dowling, 2003) which is derived from topographic modelling of a digital elevation model (DEM). An index of MRVBF < 2.7 was used to define erosional uplands (McKenzie and Gallant, 2005). A variety of DEM's were available for the individual study areas discussed in this report including radar-altimeter data acquired along with the airborne geophysics and the national-scale 9-second DEM from Geoscience Australia. Unfortunately most of the boreholes were drilled in alluvium and those defined as upland were from only two AEM survey areas at Billabong Creek and Billabung Creek, both in NSW (see Figure 9). These represent the population of suitable bores for the correlation between downhole salinity data and the gamma-ray signatures.

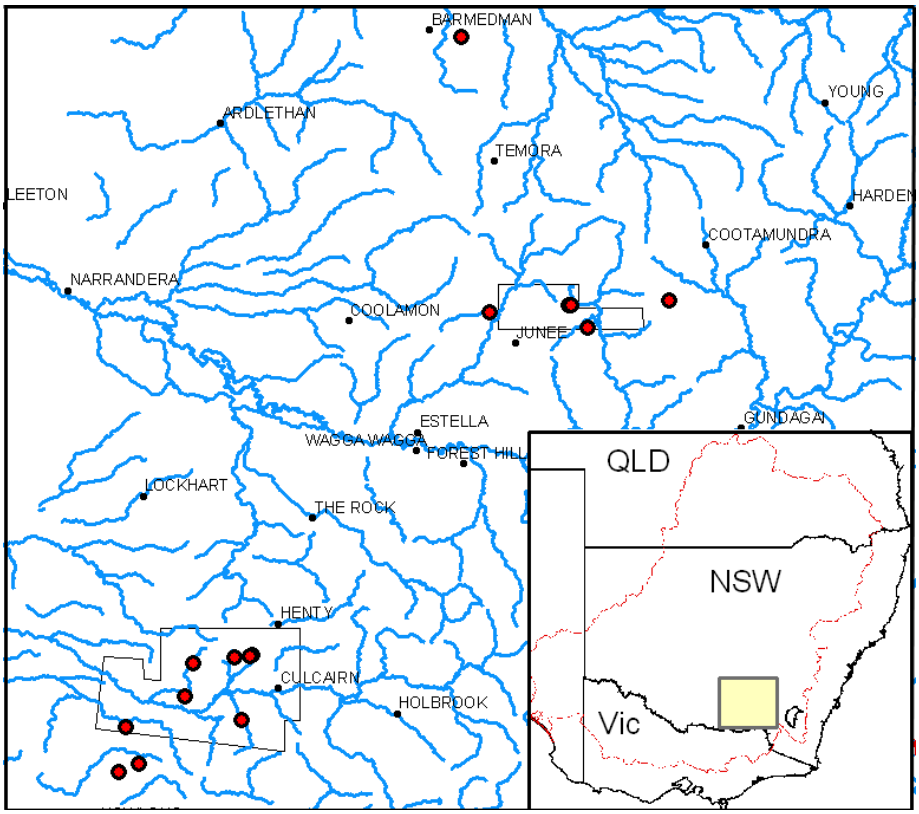

Figure 9: Location of upland boreholes produced from the MDBC airborne geophysics project

Comparison of radiometrics and downhole salinity data

A number of sources of error will be present in any correlation of airborne data with downhole readings. These include data calibration errors, differences in measurement scale and the presence of shallow alluvial cover that may mask aeolian salt-source materials (Bierwirth, 2006). Also some of the salt in boreholes is likely to be sourced from materials that are upslope from the site. To address this latter issue, regions of interest were drawn to include the area, based on the DEM, which would roughly incorporate up-slope colluvial sediments with a maximum distance of 1km.

In order to avoid calibration errors at this stage, only the boreholes from a single radiometrics data-set (at Billabong Creek) were analysed. Pixel values for gamma-element concentrations and upslope averages relating to the representative Billabong Creek boreholes and for all elements, are shown in Figure 10. These values are compared with the average EC 1:5 (soil extract) for the cover and top 15m of saprolite. This zone of saprolite was included due to the general observations of higher EC 1:5 values at this depth, interpreted to be due to salt infiltration into the weathered bedrock. A broad negative relationship is observed for both K and Th and this had been expected (particularly for K) based on the earlier observations. The airborne U data is less clear and this could be due to the large errors introduced from low-count noise that is commonly a problem for this element. The relationships are likely to improve by the collection of ground-based gamma-ray measurements with better spatial resolution and longer counting times.

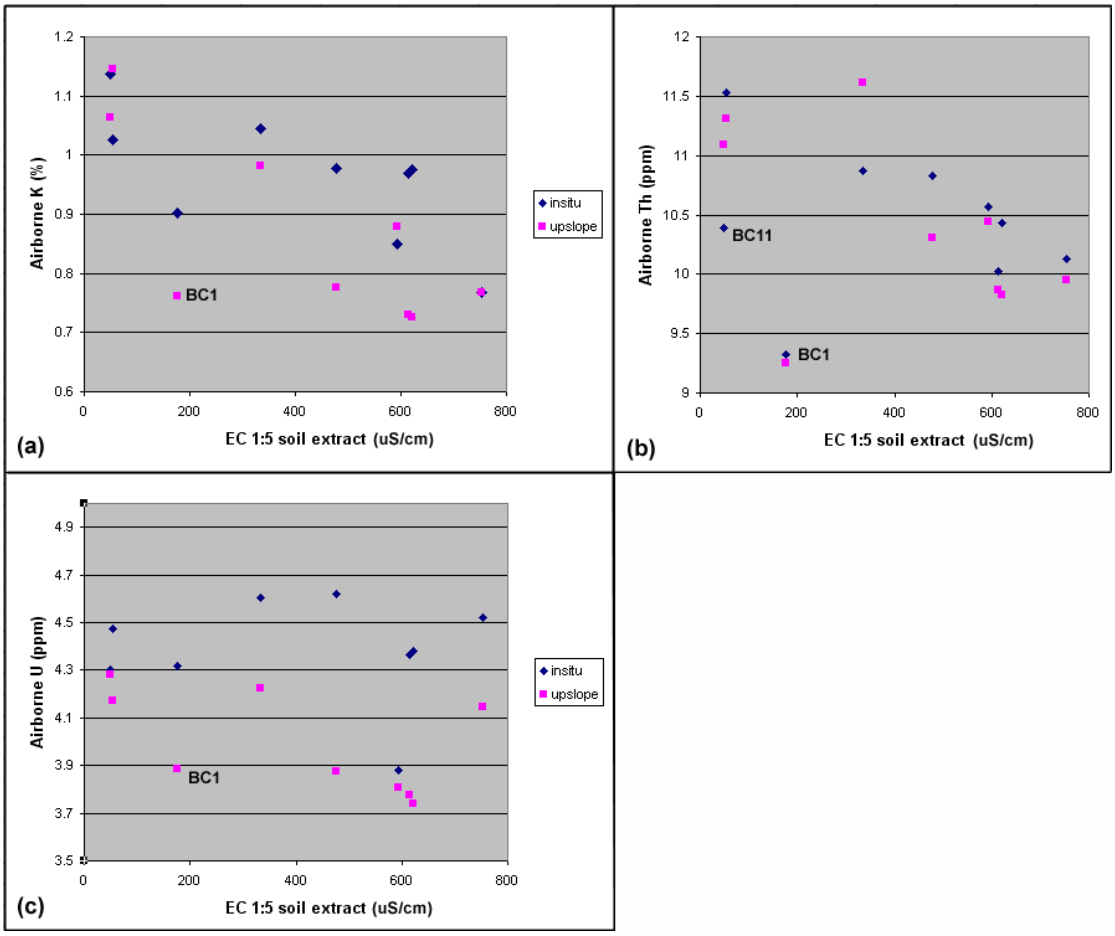

Figure 10: (a) Airborne K pixels values for boreholes determined by a topographic index (MRVBF) to be in colluvial cover over saprolite versus the average EC 1:5 for the cover including the top 15m of saprolite. These are presented for both the nearest value and averaged values upslope from the borehole (b) same for airborne Th (c) same for airborne U.

The upslope values of K corresponding to each hole can be compared with insitu values (Figure 10). The upslope relationship is generally improved and these results indicate that upland salt storages can broadly be estimated using the airborne K and Th data. Some variation can be explained by geological influence on radiometric signatures. For example, borehole BC 1 is in a foot-slope area of quartz-sandstone hills and has a correspondingly low K value (similar to saline aeolian soils), particularly for the upslope area that relates to low K sandstone outcrops. These outcrops are the purple areas in the southeast of the K image at Billabong Creek (Figure 11b), refer to the geology unit Dls1 in Figure 16 below. The same site has a low Th value relating to the quartz sand content, and this is much lower than the aeolian saline soils. Conversely one site with low salinity in metasediments (BC 11) has a similar Th signature to aeolian soils but a contrasting K signature. With the data trends in Figure 10, it appears possible to derive an index from K and Th that might separate low-salinity sandy soils from highly-saline aeolian soils.

3.5 Generating a salt source model

As mentioned earlier, McKenzie and Gallant (2005) used a low airborne K threshold and DEM-derived indices to map soil classes associated with aeolian materials that are likely to be strongly associated with salt sources. Figure 11 shows the results of their soil model in comparison with the K image. The model incorporates the MRVBF terrain variable, derived from the DEM, which effectively separates alluvial soils from upland areas that contain

aeolian materials. In the upland areas, the aeolian classes are defined using K < 111 counts per second (cps) and slope < 6% while erosional classes are primarily defined by K > 111 cps or slope > 6% (McKenzie and Gallant, 2005).

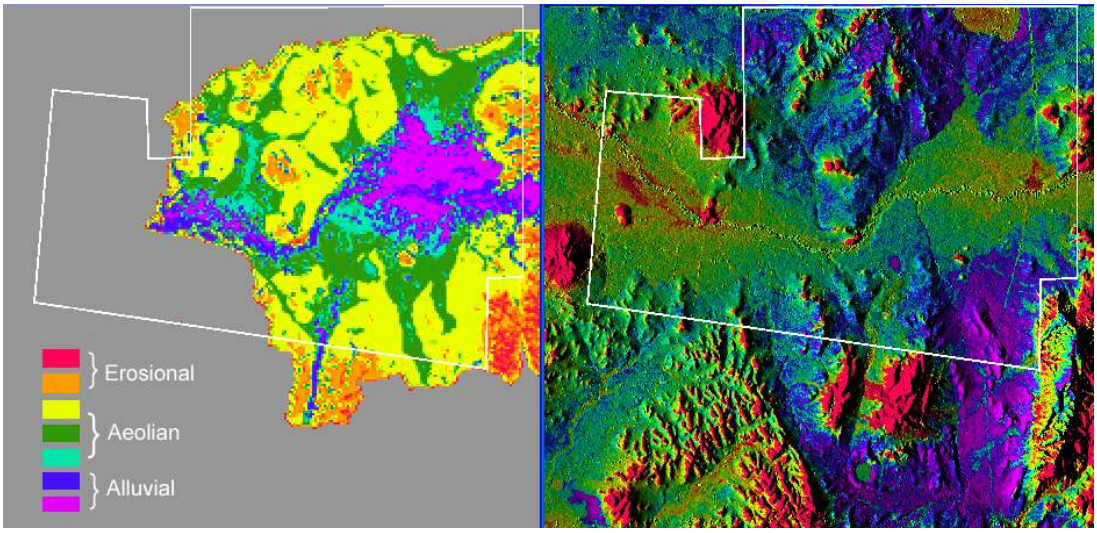

Figure 11: (a) Soil model derived from K and DEM indices (from McKenzie and Gallant, 2005) – spatial resolution is degraded compared to the original data (b) K image draped on the DEM. The white outline on both images is the extent of the Airborne EM data discussed later.

One problem with this method is that aeolian soils and certain geology types (such as quartz-sandstones in the Billabong Creek area) have overlapping K signatures. The quartz-sandstone erosional areas appear to be well defined as very low thorium values since quartz-sandstones are relatively free of thorium accessory minerals compared to aeolian dust that has moderately high thorium (presumably attached to iron oxides). These sandy soils are falsely identified as aeolian soils by McKenzie and Gallant (2005) (Figure 11a), indicating that the use of a threshold of 6 degrees for slope is inefficient at separating the classification for sandstone areas (outcrop and colluvium) from residual aeolian landscapes.

Apart from masking the mapped sandstone areas, the problem can be overcome by incorporating the thorium data into a potential model. One simple model is achieved by calculating the Euclidean distance (E_D):

$$E_D = \sqrt{((K_i - K_t)^2 + (Th_i - Th_t)^2)} \quad (1)$$

where (K_i Th_i) are the radiometric data values for i^{th} pixel and (K_t Th_t) is the target value for the saline aeolian soils end-member. Prior to this calculation, the K data was transformed so that the mean and standard deviation equalled those for the Th data. A target value of 0.7% K and 10ppm Th for saline aeolian soils were obtained from Figure 10. These are similar to the thresholds used by Dickson and Scott (1998) to characterise aeolian soils in the Blayney district. Using equation 1 above, E_D was calculated and pixel values extracted for upland boreholes for both the Billabong Creek and Billabung Creek areas (see Figure 9 for location). These were plotted against EC 1:5 (soil extract) data which were averaged for the cover material including the top of the saprolite (Figure 12). In general there is a much better correlation between E_D and upland salinity than for the individual elements K and Th, as depicted in Figure 10. Apart from the borehole BC1, whose distance appears to be still

influenced by the gamma-ray signature of sandstone soils, pixels with a Euclidean distance (to the target signature) of less than 1 generally have an EC 1:5 (soil extract) > 400 uS/cm, a value that, although not quite a saline soil, represents a substantial salt-source.

The data in Figure 12 indicates that the Euclidean distance algorithm could work in a broader exercise to define salt sources across the Murray-Darling Basin. The model was then applied to the basin wide mosaic (Figure 13). Using the linear relationship between E_D and EC 1:5 from Figure 12, the available radiometrics E_D data for the basin were calibrated to EC 1:5 of the soil for upland areas. Two discrete classes were then created using EC 1:5 thresholds:

Class 1 = EC 1:5 (soil extract) > 430 uS/cm (red in Figure 13)

Class 2 = 350 < EC 1:5 < 430 (orange in Figure 13)

The remaining classes were < 350 uS/cm and given a class based on the simplified geology of the Murray-Darling Basin (Kingham, 1998). Of the upland geology-types, basalts, quartz sandstones and limestones (Figure 13, magenta) may have signatures that are closer to the aeolian salt-source materials than granites, acid-volcanics and clay-rich sediments (green). Alluvial areas were derived from the MRVBF topographic index (Gallant and Dowling, 2003).

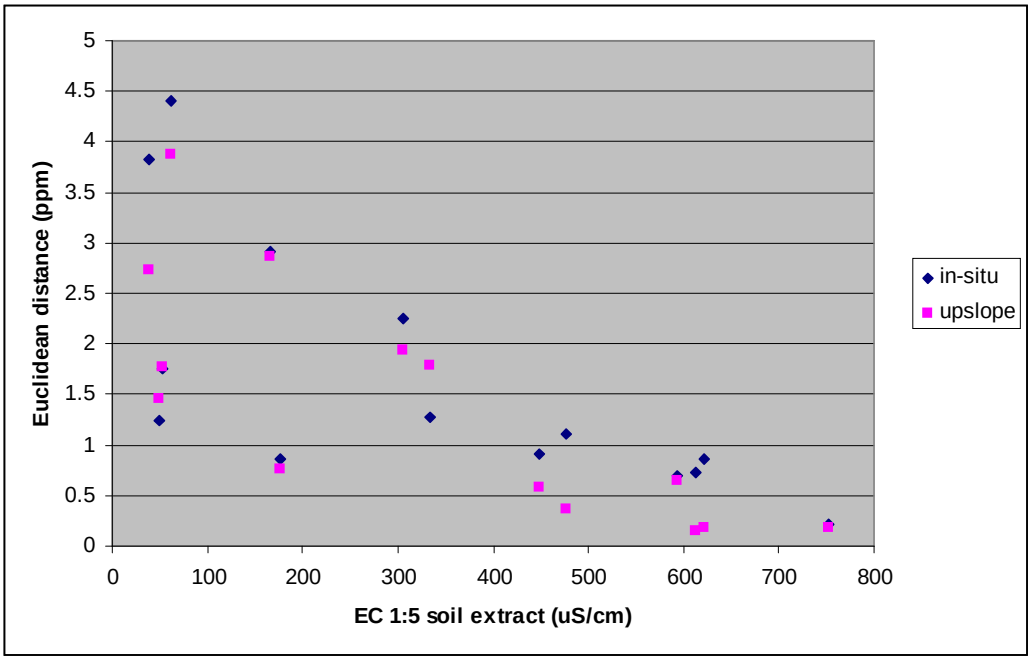

Figure 12: Correlation between EC 1:5 of the soils in upland boreholes to the Euclidean distance from pixel values to a specified target value of K and Th for saline aeolian soils.

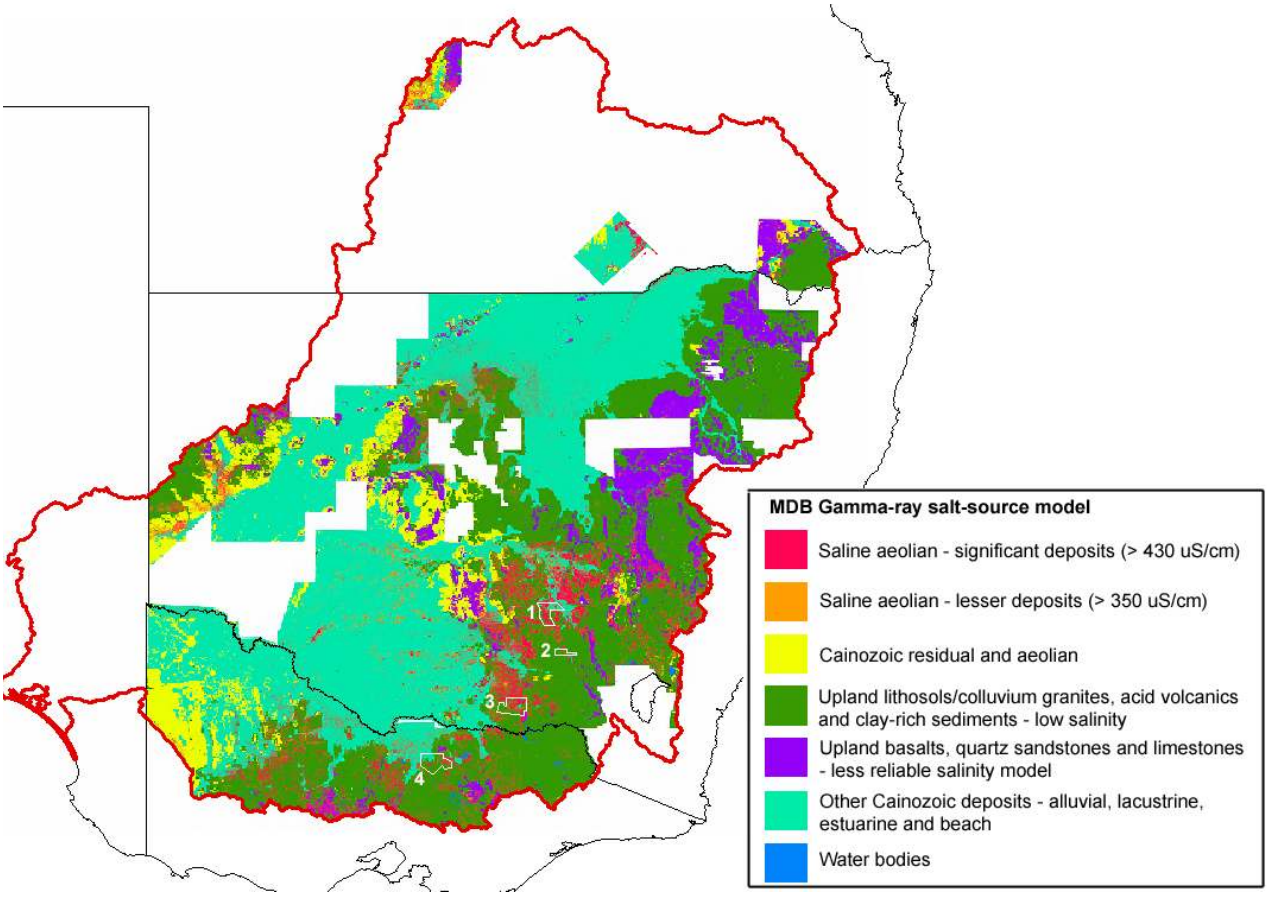

Figure 13: Salt source model image of the Murray Darling Basin. White outline areas are AEM survey areas: (1) Gilmore (2) Billabung Ck, (3) Billabong Ck and (4) Honeysuckle Ck.

The major area of saline aeolian materials derived from the radiometric analysis forms a fragmented arcuate body stretching from northern Victoria to north-central NSW (Figure 13). This fits with dominant westerly wind paths sourcing material from the inland arid parts of the Murray Geological Basin (Figure 3). Figure 15 shows the distribution of the modelled aeolian deposits downwind of the ancient Lake Bungunnnia and the dunefields and playa lakes that make up the landscape in this area today. Aeolian deposition occurs when the dust plume encounters decreasing wind velocity or turbulence due to changes in land surface roughness (such as vegetation or hilly terrain) or wash out due to rainfall (Pye, 1984). The arcuate distribution along the eastern flank of the basin corresponds to where the topography becomes more undulating, vegetation more significant and rainfall higher, when compared with the flat arid landscape to the west. Examination of the relationship with elevation (Figure 14) shows that the modelled aeolian deposits actually lie in a broad region with geomorphic similarity, i.e. lower western slopes of the Great Dividing Range. This similar geomorphic position suggests that all this mapping with a similar gamma signature is the same material. Also, the topographic high which extends in a northwest direction into the basin appears to acting as a trap for aeolian material accounting for the most intense accumulation just north of centre in the image (Figure 14).

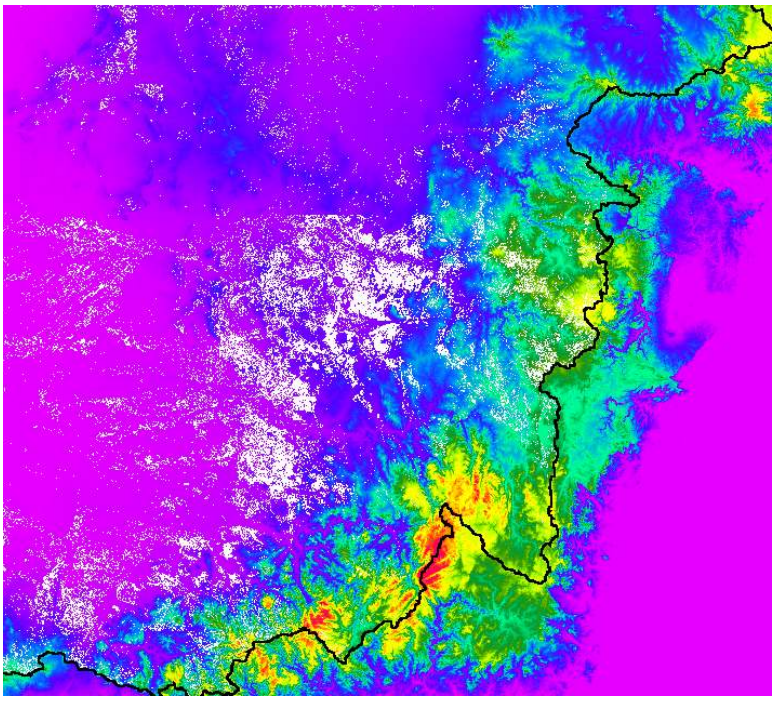

Figure 14: Comparison of salt source model image (white) with DEM

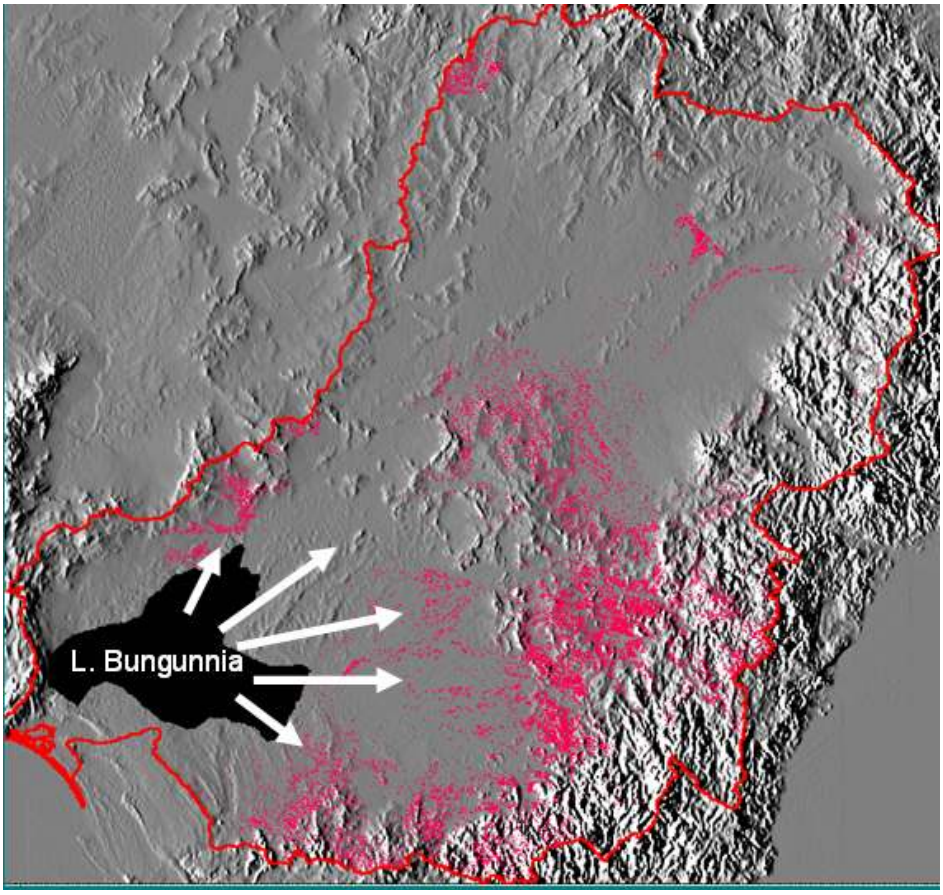

Figure 15: Aeolian salt-sources (red) in the MDB overlain on a hill-shaded DEM (Shuttle Radar Topography Mission – sourced from NASA) in relation to the ancient Lake Bungunnia.

4. Comparison with AEM study areas

As discussed earlier, there are a number of previous studies that recognise aeolian dust deposits and their associated gamma-ray signatures (Dickson and Scott, 1998; McKenzie and Gallant, 2005). As shown in Figure 12, borehole data suggests that these aeolian deposits and soils with these gamma-ray signatures have elevated salt contents. As discussed earlier, these boreholes were associated with airborne EM surveys conducted as part of the MDBC airborne geophysics project (Dent *et al*, 2003). This project concluded that in most areas the airborne EM data provided information on spatial salt stores in three dimensions throughout the landscape. It seems logical that if the gamma radiometrics, as asserted here, shows locations of salt sources, there should be an observable relationship between the radiometrics-based mapping and the airborne EM data. The following sections examine this relationship for individual AEM survey areas.

4.1 Billabong Creek

The Billabong Creek AEM survey area is shown outlined in the bottom-left area of Figure 9. Interpretation of both the gamma-radiometrics and AEM data is discussed in detail in Bierwirth (2006). Significant aeolian deposits are mapped by McKenzie and Gallant (2005) (see Fig. 11) although these are not represented in the available geological mapping. Geological units, derived from the NSW Geological Survey 1:250,000 mapping, are shown in Figure 16. Bedrock geology consists of Ordovician metasediments of slate and phyllite (Os), Silurian granites (Sjp, Sggp) and volcanics (Slv) and Devonian sediments (Dls) that include sandstone, conglomerate, siltstone and shale.

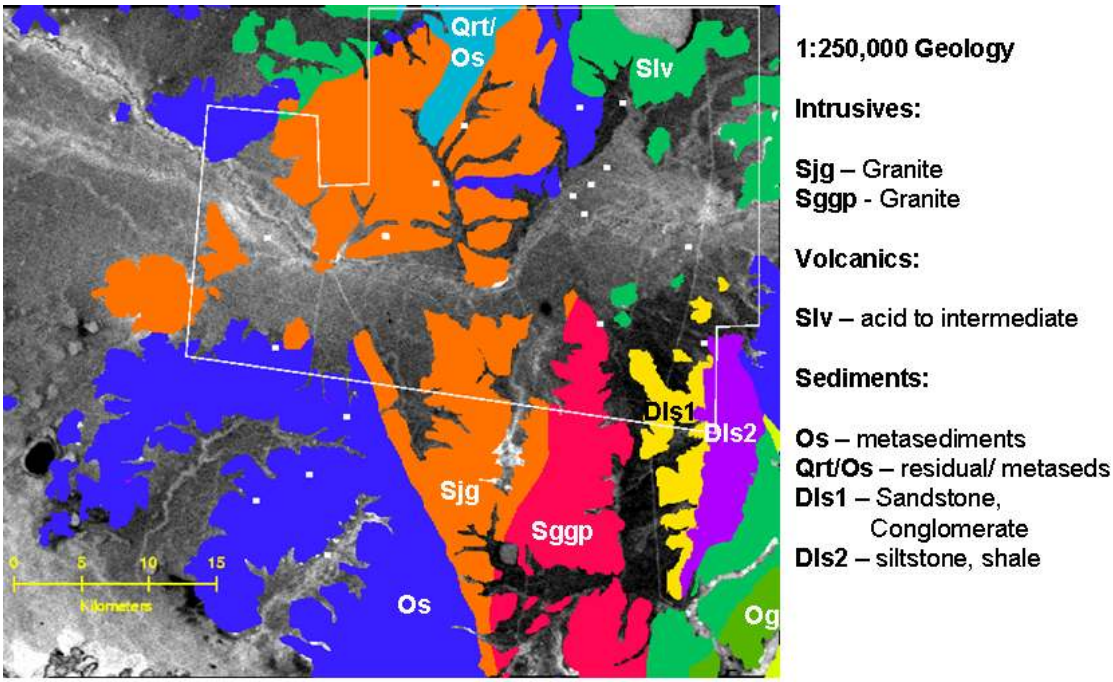

Figure 16: Geology of the Billabong Creek radiometrics survey area. The AEM survey area is shown as white and the potassium image is shown in grey tones in areas mapped as alluvial cover.

The study by Bierwirth (2006) showed that at Billabong Creek, the AEM data was poorly calibrated in two dimensions at least, i.e. vertically displaced together with the gradual decline in values at depth. Also since the highest AEM layer equates to the landscape at about 20m depth, the surface layers are effectively missing. Figure 17 shows representative layers

together with a colour composite. After shifting the AEM layers down by 20m (see Fig 12), borehole relationships show a generally good relationship between AEM conductivity, down-hole conductivities and salt (Jones *et al*, 2003; Bierwirth, 2006). As a result the AEM conductivities can be broadly calibrated to salt content (EC 1:5 soil extract) (Figure 17). The deeper salt stores such as in the Kangaroo Creek alluvial terrace (Figure 17a) can be clearly seen to be segmented but apparently connected to more extensive and shallow salt stores that are overlying saprolite (Figure 17a). This suggests that the extensive salt stores such as at Kangaroo Creek are locally-sourced which has implications for management. In general the lateral extent of salt-affected geological material increases towards the surface.

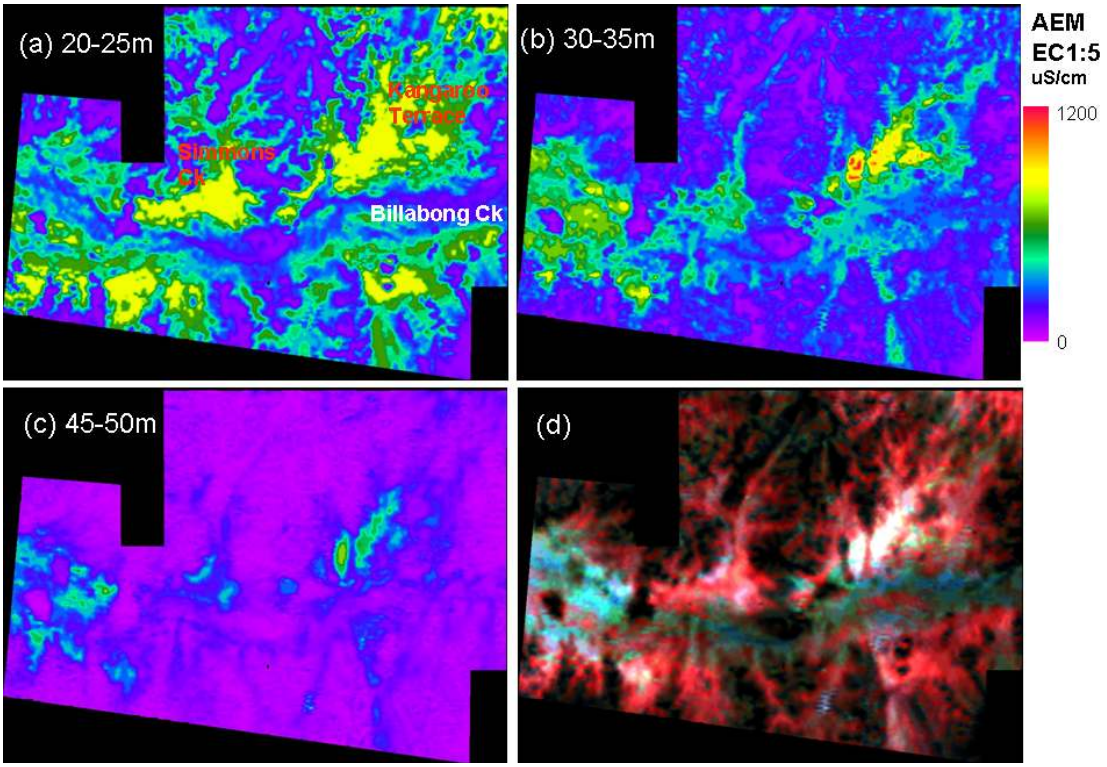

Figure 17: (a)-(c) Billabong Creek AEM data downward-shifted by 20m and calibrated to EC (d) composite of AEM depths 20-25m, 35- 40m, 45-50m as RGB respectively.

Using the assumed linear relationship between E_D and EC 1:5 from Figure 12, the radiometrics data were calibrated to EC 1:5 of the soil for upland areas (Figure 18). The resulting distribution is not consistent with geological boundaries (Figure 16), which further supports aeolian deposition. The areas of shallow salt storage defined by the AEM are also shown on Figure 18, defining a spatial relationship between upland salt sources indicated by the radiometrics and salt accumulations lower in the landscape as indicated by the AEM. The significant lowland saline areas are downslope from the upland accumulations of aeolian deposits. It is highly likely that yellow to red areas (EC 1:5 – 400 to > 700 uS/cm) in Figure 18 are major salt sources in the Billabong area. A soil with EC 1: 5 of 700 uS/cm is considered saline with respect to the viability of crops (Baskaran Sundaratnam pers. com.), although this value could be less for a material to potentially be a source for salt for later accumulations lower in the landscape.

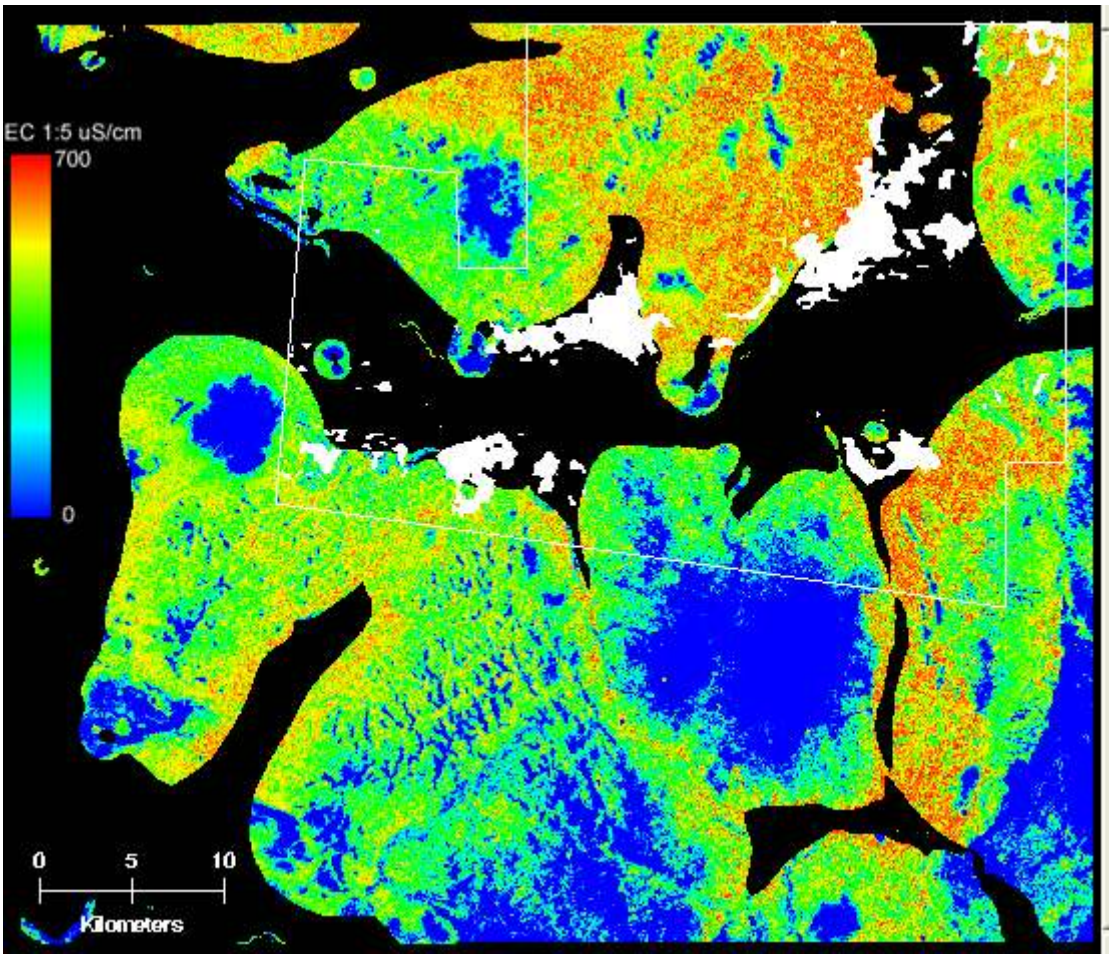

Figure 18: Upland salt model based on Euclidean distance and airborne K and Th calibrated to borehole EC 1:5 data for Billabong Creek. Black areas are alluvium defined by thresholding the MRVBF topographic index. White areas, indicating salt, are the highest values of uppermost AEM layer (20-25m).

If the upland aeolian salt model derived from the airborne radiometrics data is valid, there should be a reasonable correlation with the calibrated AEM data although the uppermost 20m of the geological profile is not effectively represented by the latter. Figure 19 shows the comparison and there is a logical spatial relationship. The AEM data (Figure 19b) shows similar levels of EC 1:5 to the salt sources defined by the gamma-ray data (Figure 19a). Interpretation of these images is based on the fact that these two geophysical methods are highlighting two fundamentally different aspects of the conceptual model. The gamma-radiometric model shows the extensive near-surface deposition of aeolian salt-source materials in the upland areas. The AEM data is highlighting the deeper zones where salt is being mobilised and directed down-gradient to the significant accumulations in the floodplain as indicated in Figure 18. As an example, very little aeolian material is evident in the southern central uplands of the survey area as indicated by blue in Figure 19a. In this area there is no significant deeper saline zones (Figure 19b) directed towards any nearby salinity accumulations in the floodplain (Figure 18).

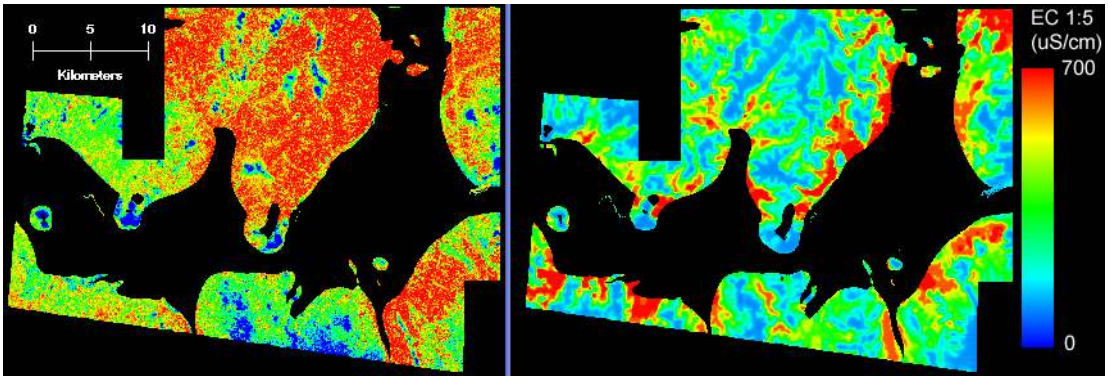

Figure 19: Comparison of calibrated salt models for Billabong Creek derived from (a) airborne K and (b) the airborne EM.

4.2 Billabung Creek

The Billabung Creek catchment encompasses some 10,000 hectares on the Southwest Slopes of New South Wales between Cootamundra and Junee, draining to the Murrumbidgee River upstream of Wagga Wagga. The AEM was flown in this area due to high levels of salt found in Billabung Creek and the problem of this salt contribution to the Murrumbidgee River. (Braaten *et al*, 2003). In Figure 20, the AEM survey area and Billabung Creek are shown in relation to the Murrumbidgee River. The area within the fly-zone is gently undulating with a generally low radiometric-K signature which suggests that there could be significant aeolian sediments here as well.

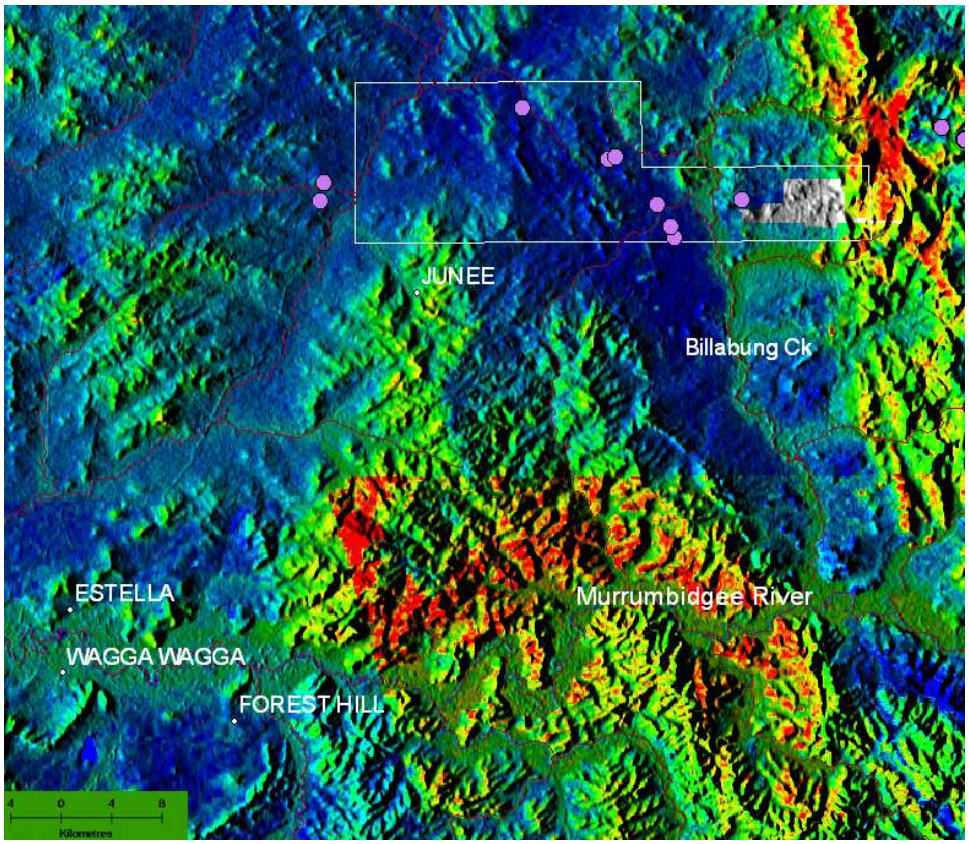

Figure 20: A mosaic of airborne potassium showing Billabung Creek, the AEM fly-zone (white outline) and boreholes in relation to the Murrumbidgee River and Wagga.

The surficial geology (Figure 21), although coarsely mapped, consists of sedimentary rocks (siltstones), metasediments, acid and basic volcanics, granitoids and mapped alluvium.

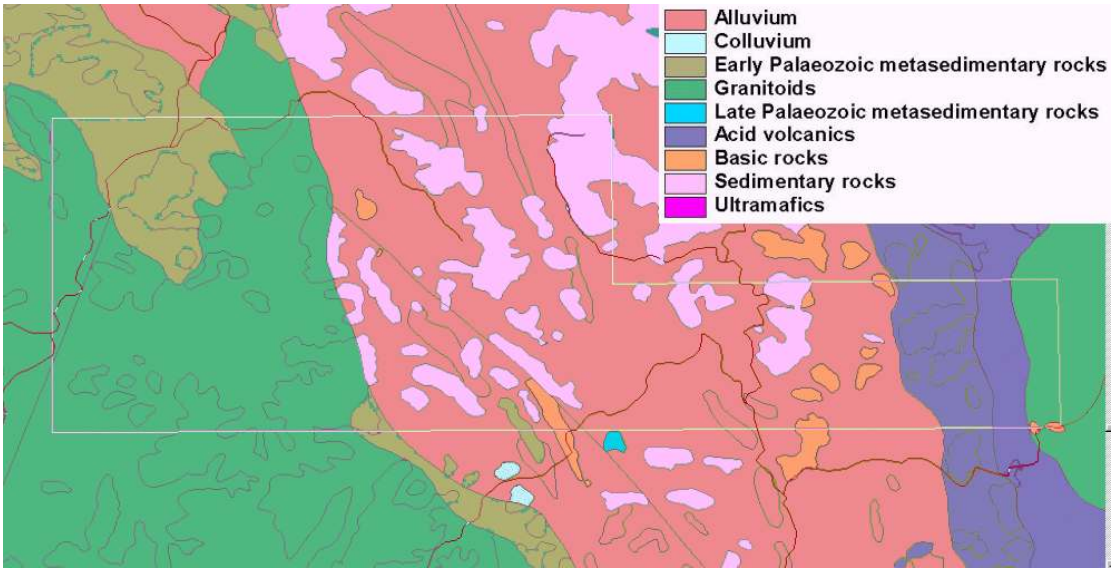

Figure 21: Geology of the Billabung Ck AEM survey area. From NSW geological survey 1:250,000 mapping.

Braaten *et al* (2003) found that salt stores are quite localised within the landscape. Salt is associated with different geological formations and landforms in different areas, but generally, with thick clay soils and regolith (unlithified sediments such as alluvium, and weathered material overlying hard rock). These are the hallmarks of aeolian deposits being a significant component of catchment salt storage.

The gamma-radiometrics salt source model (Figure 22a) shows a close visual correlation with the near-surface AEM data (Figure 22b), with red and orange colours in both images related to salt. This is remarkable given the independence and vastly different nature of these two datasets. Close comparison of these features with geology (Figure 21) indicates that the surficial salt zones are transgressing the different lithologies and are unlikely to be related to bedrock materials. The significant aeolian classified soils (red in Figure 22a) are overlain on the AEM data in Figure 22(c) and this demonstrates the good spatial correlation. This class appears to lie in low slope areas and this would be expected with the topographic position of significant aeolian materials on residual landscapes.

Like Billabong Creek, the correlation between gamma-radiometrics and AEM data is significant. Given that the AEM shows us generally the location of salt stores and the radiometrics is identifying original salt-sources, this means that the AEM can now be interpreted as to which part of the salt store has moved relative to the salt source. If this is generally applicable over wide areas of the Murray-Darling Basin, this combination of technologies is extremely important for salinity assessment and management.

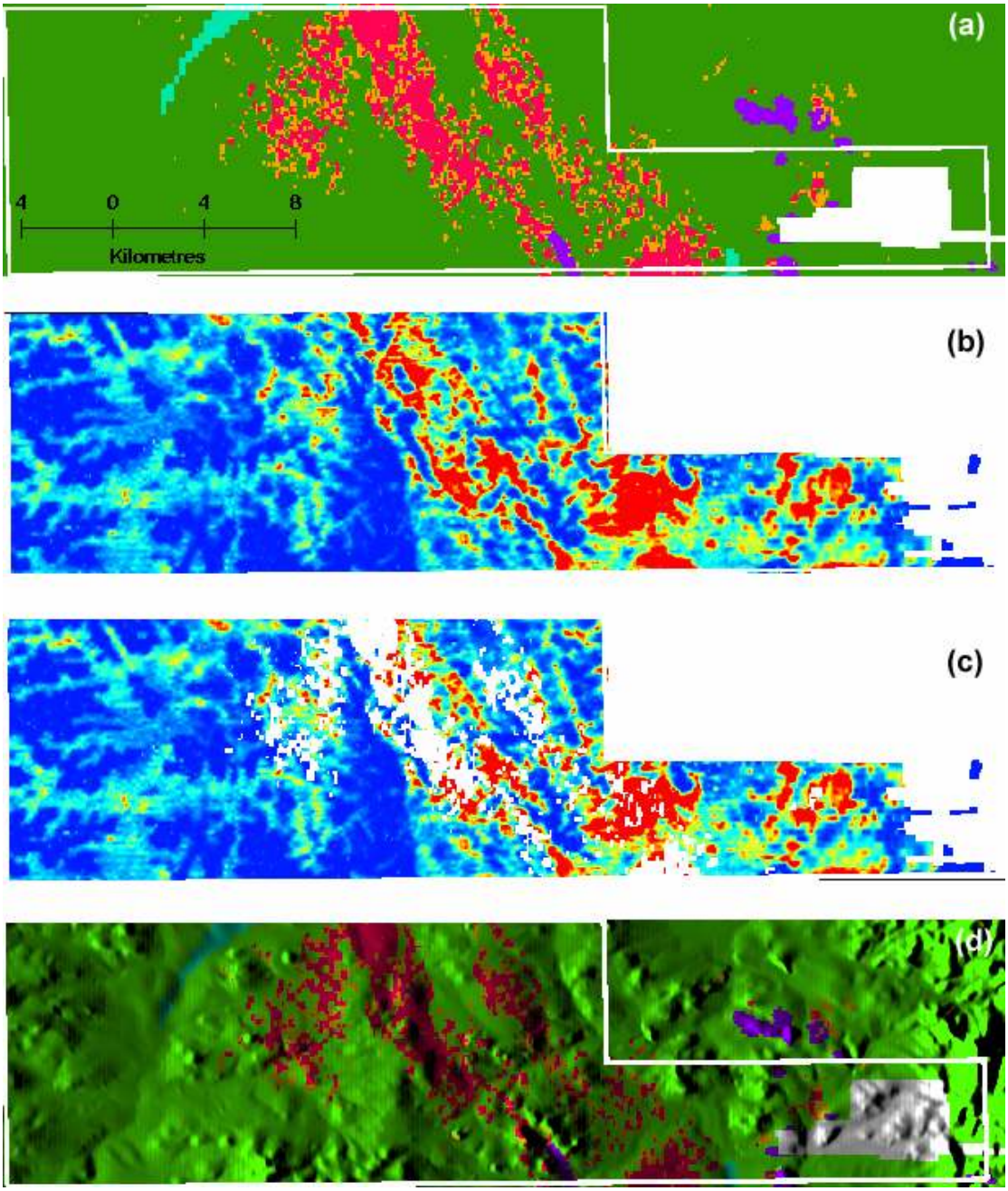

Figure 22: Billabung Creek AEM fly-zone. (a) gamma-ray salt source model (b) AEM conductivity layer 10-15m (c) AEM layer 10-15m with high gamma model salt source (red from Figure a) overlain in white and (d) The salt source model overlain on a shaded relief DEM.

4.3 Honeysuckle Creek

In contrast to the Billabong Creek AEM data, the Honeysuckle Creek survey is well calibrated (Christensen, 2003). The survey area consists largely of alluvium with a low range of hills consisting of Ordovician metasediments that can be seen in the DEM (Figure 23d). None of the investigation boreholes for this area were located in upland areas so there is no data on salt source materials. However, the AEM data (0-10m, Figure 23a,b) shows high and shallow salt-related conductivity in the area of low hills, generally in the low slope cover between the ridges (English *et al*, 2004). At deeper levels (Figure 23c) these areas have less conductivity and low salt associated with the saprolite of the metasediments. At 15-20m depth, the salt is concentrated in alluvium further to the northwest and often appears to be associated with magnetic paleo-channels that are pathways for salt movement (Dent, 2003).

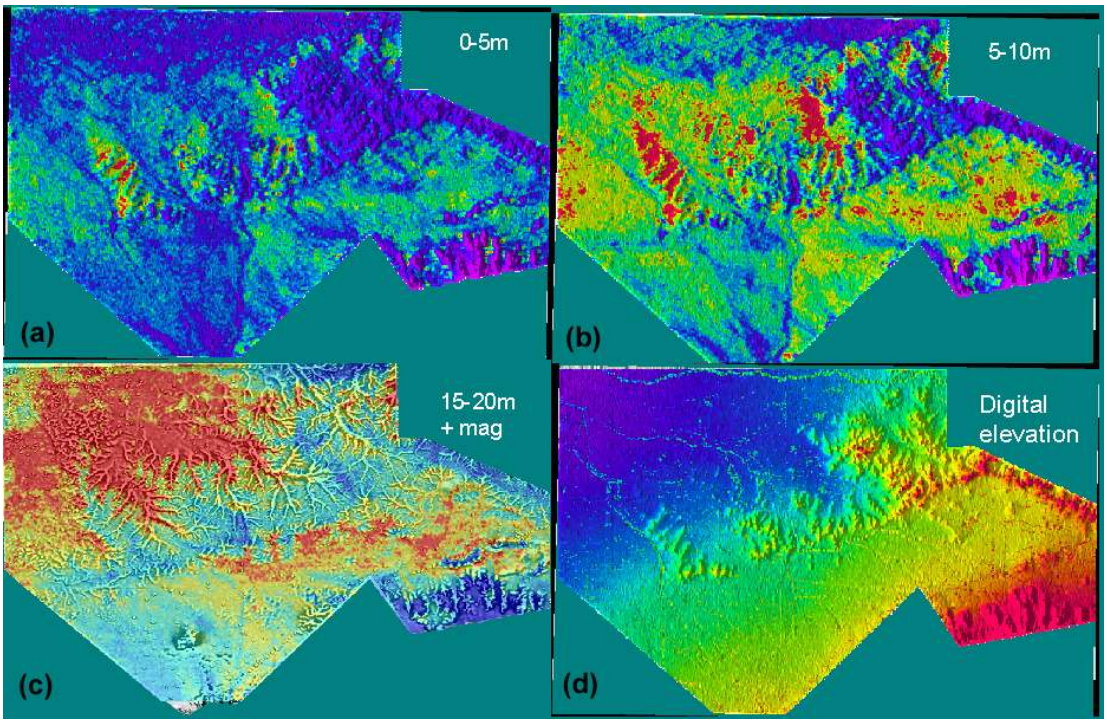

Figure 23: Honeysuckle Creek AEM layers for (a) 0-5m (b) 5-10m (c) 15-20m with magnetics 1st vertical derivative as intensity and (d) elevation in colour with shaded relief as intensity. Red is high, blue low.

Similar to the Billabong Creek and Billabung Creek survey areas, the comparison of the gamma salt-source model with the 0-5m AEM layer shows a correlation (Figure 24). Importantly, the modelled aeolian deposits (white in Figure 24b) correspond with the shallow salt areas along the range of low hills (c.f. Figure 23a). The data can be interpreted to indicate initial salt stores in these upland areas with significant mobilisation to deeper alluvium to the northwest directed by the palaeochannel network. Although it appears that much of this salt has been mobilised, these source areas would still require appropriate management.

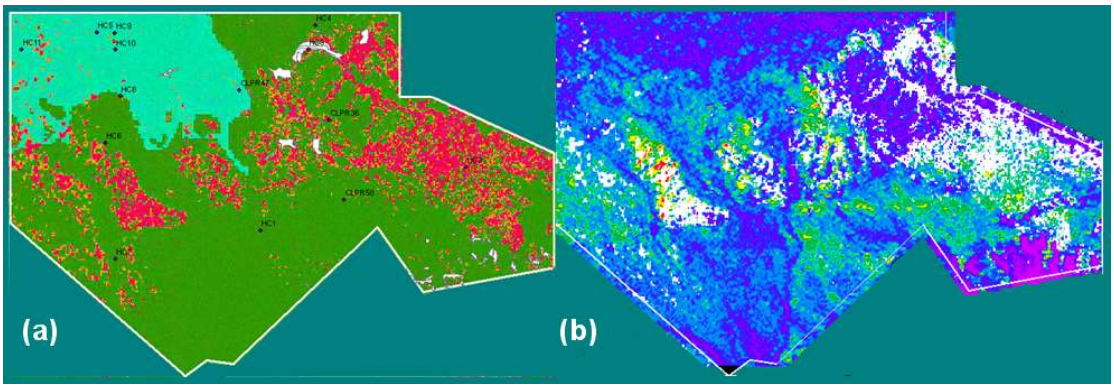

Figure 24: Comparison of the (a) gamma-ray salt source model (mapped salt scalds are overlain in white) with (b) the surface layer of AEM for Honeysuckle Creek (red values from the salt source model are overlain in white).

5. Discussion and Conclusions

The evidence presented suggests that it is possible to broadly map salt-sources across large parts of the Murray Darling Basin using airborne gamma-radiometrics. This is supported by both drillhole data and correlation with airborne EM surveys, a technique that has been demonstrated to detect salt stores in the landscape. A conceptual model based on surficial aeolian deposits as being a significant salt store forms the basis of the mapping. Such a mechanism has been proposed in previous investigations of dryland salinity including Acworth *et al* (1997) and Evans (1998). Such aeolian deposits have been identified across many upland catchments in the Murray-Darling Basin including Billabong Creek (McKenzie and Gallant, 2005), Wagga Wagga (Chen, 2001) and Young (Chartres *et al*, 1988).

Features of the mapping derived from the gamma-radiometrics also support the underlying conceptual model. Much of the modelled aeolian materials lie in a similar landscape position and do not coincide with geological boundaries. It could be argued that this relationship with geomorphology just indicates a weathering zone. However it also fits the aeolian model where a broad region in the foot-slopes of larger mountains might be the expected accumulation zone for windblown materials. This, when combined with multiple observations of aeolian materials in soil profiles, provides strong evidence for the validity of the gamma-ray salt-source model.

The geographical relationship between the saline aeolian deposits, forming an arcuate shaped pattern around and to the east of the ancient Lake Bungunnia and its arid hypersaline equivalents (Figure 15) is also persuasive in explaining the mechanism of formation of salt source zones in the MDB. Clearly the grainsize of aeolian deposits will depend on the distance travelled from the source, ranging from proximal sands observed in the Murray Basin (see Figure 5) to silts and to predominantly clay sized particles that eventually fall into the Tasman Sea (Hesse, 1994), refer Figure 3. The saline aeolian materials modelled here have a bi-modal distribution of particles being both clay and silts (see Figure 2). This would be expected where windborne silt-sized clay pellets (containing salt and derived from salt lakes) are mixed with other silts (containing iron oxides and derived from weathered plains interstitial to the lakes). Subsequent disaggregation of the clay pellets will result in clay-sized particles, giving the bimodal distribution that is commonly observed. This could mean that salt may only be present in the silt sized particle range of aeolian deposits as represented by the salt-source materials mapped by the gamma-ray model presented here. The other size fractions of aeolian deposits (eg sand dunes) are likely to have different mineralogy and hence different radiometric signatures.

The gamma-ray signature of the modelled saline aeolian deposits can be partly explained by the discussion above. Salt lake materials would generally be expected to have low potassium and thorium, but these materials mixed with weathered lake-interstitial iron-oxide-rich silts could produce the observed signature. These latter silts are likely to have a low potassium concentration due to weathering and a higher thorium value due to the complexing of thorium with Fe-oxides (Dickson and Scott, 1998). This would result in a general low K and mid-range Th that is the observed signature.

The new work presented here also brings into question the magnitude of the effect of weathering on gamma-ray signatures. An original work on this effect (Bierwirth, 1996) suggested that significant element loss, particularly K, occurred in the weathered soils relating to many lithologies. From the current work, it appears that at in at least some of these areas, aeolian materials were contributing to the low K signatures. In the metasediment areas near Wagga Wagga, the thorium response remained elevated even in the weathered zones and it was assumed that Th remained as a residual (Bierwirth, 1996). However, given the now known radiometric response of aeolian materials, the presence of significant aeolian materials

is now an alternative explanation. Despite this it is still logical that weathering contributes to element loss and in some cases enhancement.

The model presented here only partially accounts for reworking of aeolian materials and the potential mixing of their gamma-ray signatures with those of bedrock. The Euclidean distance algorithm allows for partial mixing with colluvial and alluvial sediments depending on what distance-threshold is used. The most rigorous application would use geological boundaries and characteristic lithology signatures to unmix the aeolian component, although accurate geological boundaries are often not available. Nevertheless, the current model, that does not incorporate geology, appears to be working well.

Although not available for this study, chemical analyses including isotopes would be very valuable for attempting to provide a sampling signature for aeolian soils. It may be that some of these target materials are depleted in terms of their original salt storage and this is important information for management. Soil and water chemistry may also be an important tool for verifying whether the gamma-ray salt-source model is mapping aeolian or other geological materials like sandstone or basalt colluvium.

In terms of management, the new model adds an extra dimension to existing geophysical techniques. While the AEM data has proved valuable in understanding where the salt stores are in the landscape, magnetics data has often showed subsurface paleochannels and pathways for salt movement often for a considerable distance. The gamma model appears to show the component of the AEM that represents the major source of the salt. In this way the AEM can be further interpreted as to which part of these data represent mobilised salt. This is highly significant in terms of management.

As radiometrics data is widely available, the technique is a cost-effective addition to the current tools. AEM has proved a contentious tool largely because of the large costs involved. The gamma model is a method that can be readily and synoptically applied over large areas. The experience of interpreting the gamma-ray salt source model with a number of existing AEM data-sets means that it may be possible to predict where salts are and what an AEM survey might look like where it currently does not exist.

5.1 Further work

The model presented here covers a large geographical area that includes a variety of geological and geomorphic environments. As such there are many issues and a number of aspects of further work are recommended.

The identification of aeolian soils can be difficult, particularly when they are weathered or mixed with other material. This requires research to investigate the relationships between gamma-ray signatures, aeolian soils and other geological materials.

Clearly the map needs to be validated further to provide confidence in its use in facilitating better management of dryland salinity. Verification will require:

(i.) Analysis of available ground truth data such as stream and groundwater monitoring and drillhole information;

(ii.) Collection of new data such as field gamma-ray spectrometry, drilling and laboratory analysis of the chemistry of soils and regolith.

Some existing radiometrics data, particularly for South Australia, is yet to be acquired for the model. Also the issue of radiometric calibration is not trivial. As mentioned earlier, a large number of the 94 surveys used so far have calibrations that are not consistent. While this has been largely corrected in the mosaic generated here, significant adjustments should be made to improve the model.

6. Acknowledgements

The authors would like to thank Peter Baker, Emma Lawrence and Baskaran Sundaram from the Bureau of Rural Sciences for their various contributions to this work.

7. References

Acworth, R.I., Broughton, A., Nicoll, C. and Jankowski, J. (1997). The role of debris-flow deposits in the development of dryland salinity in the Yass River catchment, NSW, Australia. *Hydrogeology Journal*, 5(1), 22-36.

An, Z., Bowler, J.M., Opdyke, N.D., Macumber, P.G. and Firman, J.B., (1986). Paleomagnetic stratigraphy of Lake Bungunnia: Plio-Pleistocene precursor of aridity in the Murray Basin, southeastern Australia. *Palaeogeography, Palaeoclimatology, Palaeoecology* 54, 219-239.

Beattie, J.A. (1972), Groundsurfaces of the Wagga Wagga region, New South Wales. *CSIRO Soil Publication* No. 28.

Bierwirth,P.N,. Gessler,P. and McKane, D. (1996), Empirical investigation of airborne gamma-ray images as an indicator of soil properties - Wagga Wagga, NSW. *8th Australasian Remote Sensing Conference Proceedings*. Canberra.

Bierwirth, P.N. (1996), Investigation of airborne gamma-ray images as a rapid mapping tool for soil and land degradation - Wagga Wagga,NSW. *AGSO Record 1996/22*.

Bierwirth, P.N., (2006), Defining sources and stores of salt at Billabong Ck, N.S.W, using airborne gamma-radiometric and electro-magnetic data. *BRS Report*, Bureau of Rural Sciences, Canberra.

Bowler, J.M., (1976), Aridity in Australia: Age, origins and expressions in aeolian landforms and sediments. *Earth Science Review*, 12, 279-310.

Bowler, J.M., (1983), Lunettes as indices of hydrologic change: a review of Australian evidence. *Proc. Ro. Soc. Vic.* 95/3, pp 147-168.

Bowler, J.M. and Wasson, R.J. (1984), Glacial age environments of inland Australia. In: Vogel JC (ed) *Late Cainozoic palaleoclimates of the Southern Hemisphere*. AA Balkema Rotterdam, 183-208.

Braaten, R., Baker, P., and Dent, D.L. (2003) A systems approach to salinity management at Billabung Creek, New South Wales. *BRS Report*. Bureau of Rural Sciences, Canberra.

Brown, C.M. and Stephenson A.E. (1991), Geology of the Murray Basin, southeastern Australia. BMR Bulletin 235. Bureau of Mineral Resources, Geology and Geophysics, Canberra.

Butler, B.E. (1956), Parna- an aeolian clay. *Australian Journal of Science* 18, 145-151.

Butler, B.E. and Hutton J.T. (1956), Parna in the Riverine Plain of south-eastern Australia and the soils thereon. *Australian Journal of Agricultural Research* 7, 536-553.

Chartres, C.J, and Chivas, A.R. (1987). The identification of aeolian additions in a soil developed on granite in south-eastern Australia. In: Liu Tungsheng (ed) Aspects of loess research. China Ocean Press, Beijing.

Chartres, C.J., Chivas, A.R., Walker, P.H. (1988), The effect of aeolian accessions on soil development on granitic rocks in south-eastern Australia. *Aust. J. Soil Res.*, 26, 17-31.

Chen, X. Y. (2001), The red clay mantle in the Wagga Wagga region, New South Wales: evaluation of an aeolian dust deposit (Yarabee Parna) using methods of soil landscape mapping. *Aust. J. Soil Res.*, 2001, 39, 61–80.

Christensen, (2003), Calibration of Honeysuckle Creek Conductivity Depth Imaging. *Australian Society of Exploration Geophysicists Preview*, 27-30.

Churchward, H.M., (1963), Soil studies at Swan Hill, Victoria. *Aus J. Soil Res* 1, 242-255.

Crowley, G.M. (1994). Quaternary soil salinity events and Australian vegetation history. Quaternary Science Reviews 13, 15-22.

Dent, D. (2003), MDBC Airborne Geophysics Project: Final Report, Bureau of Rural Sciences, Consultancy D 2018.

Dickson, B.L., and Scott, K.M. (1998) Recognition of aeolian soils of the Blayney district, N.S.W: Implications for mineral exploration. *Journal of Geochemical Exploration*, 63, pp 237-251.

Elliot G.L. and Holman, G.J. (1985), Sodium accession in rainfall near Scone Mountain, NSW. *Aus. J. Soil Res*., 23, 315-318.

English, P., Richardson, P. and Stauffacher, M. (2002), Groundwater and salinity processes in Simmons Creek sub-catchment, Billabong Creek, NSW. CSIRO Land and Water, Canberra Technical Report 24/02.

English, P., Richardson, P., Glover, M., Cresswell, H. and Gallant, J. (2004), Interpreting airborne geophysics as an adjunct to hydrogeological investigations for salinity management: Honeysuckle Creek catchment, Victoria. CSIRO Land and Water Technical Report. No 18/24.

Evans, WR. (1998), What does Boorowa tell us? Salt stores and groundwater dynamics in a dryland salinity environment. In: Weaver TR and Lawrence CR (Editors). Proceedings: International Association of Hydrogeologists International Groundwater Conference: Groundwater: Sustainable Solutions. University of Melbourne, 8-13 February, 1998: 267-274.

Gallant, J.C., and Dowling, T.I. (2003), A multiresolution index of valley bottom flatness. *Water Resources Research*, Vol., 39, no 12, 1347.

Gatehouse, R.D., Williams, I.S. and Pillans, B.J. (2001), Fingerprinting windblown dust in south-eastern Australian soils by uranium-lead dating of detrital zircon. *Aus. J. Soil Res*. 39, 7-12.

Greene, R., Gatehouse, R., Scott, K. and Chen, X.Y. (2001), Aeolian dust-implications for Australian mineral exploration and environmental management. *Aus. J. Soil Res*., 39,1-6.

Hesse, P.P., (1994). The record of continental dust from Australia in Tasman Sea sediments. *Quaternary Science Reviews* 13, 257-272.

Hope, G. (1987), Climatic implications of timberline changes in Australasia from 30 000 yr bp to present. In: Donnelly TH and Wasson RJ (eds) *CLIMANZ 3*, pp91-99. CSIRO Division of Water Resources, Melbourne.

Johnston, S.W. (2001), The influence of aeolian dust deposits on alpine soils in south-eastern Australia. *Aus. J. Soil Res* 39, 81-88.

Jones, G., Baker, P., Dent, D. (2003) Billabong Creek interpretation. In: Dent D. (ed) MDBC Airborne Geophysics Project: Final Report. Bureau of Rural Sciences, Consultancy D 2018.

Kiefert L. (1997), Characteristics of wind transported dust in Eastern Australia. PhD thesis, Griffith University, Brisbane (unpubl.).

Kingham, R.A. (1998) Geology of the Murray-Darling Basin – simplified lithostratigraphic groupings. AGSO Record 1998/21. Australian Geological Survey Organisation, Canberra.

Knight A.W., McTainsh, G.H. and Simpson, R.W., (1995). Sediment loads in an Australian duststorm: implications for present and past dust processes. *Catena* 24, 195-213.

McKenzie, N.J. and Gallant J.C. (2005), Digital soil mapping with improved environmental predictors and models of pedogenesis. In: P Lagacherie, AB McBratney,M Voltz (eds), Advances in digital soil mapping. Developments in Soil Science Series, Elsevier.

McTainsh, G.H. (1989) Quaternary aeolian dust processes and sediments in the Australian region. *Quaternary Science Review* 8, 235-253.

Melis, M.I., and Acworth, R.I. (2001), An aeolian component in Pleistocene and Holocene valley aggradation: evidence from Dicks Creek catchment, Yass, New South Wales. *Aust. J. Soil Res*, 39, pp13–38.

Olive, L.J. and Walker, P.H. (1982), Processes in overland flow – erosion and production of suspended material. In: EM O'Loughlin and P Cullen (eds), Predictions in Water Quality. Australian Academy of Science, Canberra, pp 87-121.

Pillans, B. and Bourman, R. (2001), Mid Pleistocene arid shift in southern Australia, dated by magnetostratigraphy. *Aus. J. Soil Res.*, 39, 89-98.

Pye, K.(1984), Loess. *Progress in Physical Geography* 8, 176-217.

Shackleton, N.J., Berger, A. and Peltier, W.R., (1990). An alternative astronomical calibration of the lower Pleistocene timescale based on ODP Site 677. *Transactions of the Royal Society of Edinburgh, Earth Sciences* 81, 251-262,

Stephenson, A.E. (1986) Lake Bungunnia – A Plio-Pleistocene megalake in southern Australia. *Palaeogeography, Palaeoclimatology, Palaeoecology* 57, 137-156.

Van Dijk, D.C. (1958), Principles of soils distribution in the Griffith-Yenda district NSW. *CSIRO Soil Publication* No. 11.

Wilford, J.R, Dent, D.L., Dowling, T. and Braaten, R. (2001), Rapid mapping of soils and salt stores using airborne radiometrics and digital elevation models. *AGSO Research Newsletter,* May, 2001, pp33-40, Australian Geological Survey Organisation, Canberra.

Zheng, H., Wyroll, K-H, Li, Z. and Powell, C McA, (1998). Onset of aridity in southern Western Australia – a preliminary appraisal. *Global and Planetary Change* 18, 175-187.